Travail de fin d'études et stage[BR]- Travail de fin d'études : Modelling of desiccant evaporative cooling system[BR]- Stage d'insertion professionnelle (ULiège)

Auteur : Rulot, Thibault
Promoteur(s) : Lemort, Vincent
Faculté : Faculté des Sciences appliquées
Diplôme : Master en ingénieur civil électromécanicien, à finalité spécialisée en énergétique
Année académique : 2022-2023
URI/URL : http://hdl.handle.net/2268.2/16768

University of Liege
Faculty of Applied Sciences
Academic year 2022-2023

Modelling of desiccant evaporative cooling system

Rulot Thibault s171473

Academic supervisor : Vincent LEMORT
Jury : Grégoire LEONARD & Samuel GENDEBIEN

Dissertation presented in fulfilment of the requirements for the master's degree in Electromechanical engineering by Thibault Rulot

Liege
2023

ACKNOWLEDGEMENT

I would like to thank all the people who helped me in this work and during my studies.

I would like to thank my supervisors, Alanis Zeoli and Vincent Lemort. I tank Alanis Zeoli for supporting me during this internship and allowing me to contribute to the development of her thesis. I thank Vincent Lemort for allowing me to join the laboratory for my internship.

I want to thank all the laboratory team, professors, researchers, PhD candidates and technical staff, for their hospitality and kindness.

I thank the members of the Jury for taking time to read this work.

Finally, I would like to thank my family and my friends for their support during this internship and during these five years of study.

ABSTRACT

In a context of climate changes around the world and a willingness to achieve the goal fixed, the 2015 Paris Agreement, decarbonized strategies must be established. With this climate change, an increase in cooling consumption of buildings can be expected. The current solution to achieve thermal comfort in buildings is to install air conditioning units to produce fresh air to cool the buildings. These conventional air-conditioning systems consume a relatively large amount of electricity to produce this cold, but also use refrigerants that contribute to the greenhouse effect and the destruction of the ozone layer. However, there are alternatives to conventional air conditioning, including evaporative cooling systems with a desiccant wheel.

The aim of this study is to evaluate different evaporative cooling techniques, including a review of the different possible designs and configurations. A modelling of the whole cycle for a standard configuration is performed. The modelling of each component of the cycle is addressed, a simple model for each component and a complex model for the desiccant wheel and the rotary air-air exchanger. A parametric study for each model is carried out in order to observe the impact of the evolution of the parameters on the outputs of each model. A calibration of the simple models for the desiccant wheel and the rotary air-air exchanger is carried out from data generated with the complex model as well as a validation in order to evaluate the relevance of a simple model next to a complex model. For the desiccant wheel, the simple model can substitute the complex model because the error on the desiccant wheel output is $\pm 0.5[K]$ and $\pm 0.3[g_{water}/kg_{air}]$. For the rotary exchanger, the simple model does not allow to substitute the complex model, other elements like the flow rate must be taken into account in the efficiency calculation.

This type of technology can be applied especially in hot and humid climates as it allows the regulation of both temperature and humidity to ensure optimal thermal comfort. Even more so by improving the way in which the regeneration temperature of the desiccant wheel is reached as well as by installing solar collectors in order to make the system almost autonomous in energy.

RESUME

Dans un contexte de changement climatique à travers le monde et une volonté d'atteindre les objectifs fixés, les accords de Paris 2015, des stratégies de décarbonisation doivent être mise en place. Avec ce changement climatique, une augmentation de la consommation des bâtiments en froid peut être attendue. La solution actuellement afin d'atteindre un confort thermique dans les bâtiments est l'installer des unités de climatisation afin de produire de l'air frais pour refroidir ces bâtiments. Ces climatisations conventionnelles consomment de l'électricité en quantité relativement importante afin de produire ce froid mais utilisent aussi des fluides frigorifiques qui contribuent à l'augmentation de l'effet de serre et la destruction de la couche d'ozone. Il existe cependant des alternatives à la climatisation conventionnelle dont les systèmes de refroidissements adiabatique par roue dessicante.

Cette étude a pour objectif d'évaluer les différentes techniques de refroidissements évaporatifs, notamment en faisant une revue des différents designs et configurations possibles. Une modélisation de l'ensemble du cycle pour une configuration standard est réalisée. La modélisation de chaque composant du cycle est abordée, un modèle simple pour chaque composant ainsi qu'un modèle complexe pour la roue dessicante et l'échangeur rotatif air-air. Une étude paramétrique pour chaque modèle est réalisée afin d'observer l'impact de l'évolution des paramètres sur les sorties de chaque modèle. Une calibration des modèles simples pour la roue dessicante et l'échangeur rotatif air-air est effectuée à partir de données générées par le modèle complexe ainsi qu'une validation afin d'évaluer la pertinence d'un modèle simple à côté d'un modèle complexe. Pour la roue dessicante, le modèle simple proposé peut tout à fait substituer le modèle complexe car l'erreur sur la sortie de la roue dessicante est de $\pm 0.5[K]$ et de $\pm 0.3[g_{water}/kg_{air}]$. Pour l'échangeur rotatif, le modèle simple ne permet pas en l'état de substituer au modèle complexe, d'autres éléments comme le débit doivent être pris en compte dans le calcul d'efficacité.

Ce type de technologie peut s'appliquer notamment dans les climats chauds et humides car il permet la régulation de la température mais aussi de l'humidité afin de garantir un confort thermique optimal. Plus encore en améliorant la façon dont est atteinte la température de régénération de la roue dessicante comme en installant des capteurs solaires afin de rendre le système presque autonome en énergie.

Contents

Chapter 1

Introduction

In a context of climate changes around the world and a willingness to achieve the fixed goals, the 2015 Paris Agreement, decarbonized strategies must be established. To do this, the International Energy Agency (IEA) leads through its Energy in Buildings and Communities Programme the realisation of collaborative R&D projects among its 26 members countries. Among the multitude of subject proposed by IEA-EBC, Annex 85 called Indirect Evaporative Cooling, is a project to which the University of Liège contributes through its Thermodynamics Laboratory.

For more than 30 years, the Thermodynamics Laboratory of the University of Liège has been carrying out numerical and experimental research activities in the field of thermal and energy systems.

The main subject of indirect evaporative cooling is a very broad subject, the objective of this master thesis is to develop one category of technology that is the desiccant evaporative cooling system. This technology contributes to reduce energy consumption because it offers an alternative to the conventional compression air conditioning system which is high electricity consumer. It also needs HCFCs as working fluid causing greenhouse effect and the ozone layer depletion. The desiccant evaporative cooling system is able, in addition to what the conventional air-conditioning system can do, to have the control on the humidity contained in the air injected in the room. Indeed, the humidity is also a parameter to consider to provide the human comfort indoor conditions as discussed by Rafique et al. [1].

The case study is a desiccant evaporative cooling system installed in a large office building at the Aalborg University in Denmark [2]. This building suffers from overheating in summer and intermediate seasons. Not all the building is equipped with the desiccant evaporative cooling system. The building is divided in 6 zones with dedicated HVAC systems. In the case study 2 zones are considered, one zone with a conventional ventilation system with active cooling and the second zone is equipped with the desiccant evaporative cooling system.

The objective of this paper is to perform a complete study of the desiccant evaporative cooling system. A literature review on the subject is developed, this contains some investigations on different variants possible, on modelling and on performance of such installation are developed in the section 3. The components of the cycle is modelled by a simple model. A complex modelling of the desiccant wheel and the rotary air to air heat exchanger is also performed order to evaluate the precision of the correlation proposed in the literature. A calibration and validation of the simple model is also done from data generated by the complex model. Finally, the results of the model are analysed and discussed for further applications of such installation.

Chapter 2

System description

The description of the system is carried out in this section by describing the components of the system and the different state point of the cycle.

A desiccant evaporative cooling system in a technology used in air-conditioning with two different functions. These function are sensible air cooling and dehumidification, corresponding to latent load. A scheme of the studied desiccant evaporative cooling system is shown in **Figure 2.1**.

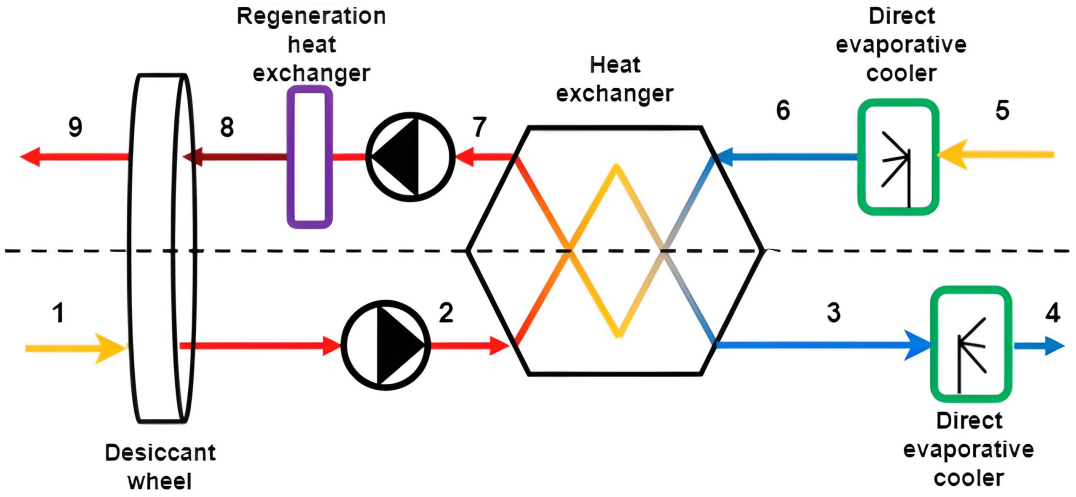

Figure 2.1: Desiccant evaporative cooling system scheme [2].

This system contains different components :

- the **desiccant wheel** used to absorb the moisture from the air;
- the **heat exchanger** which allows to transfer the heat injected in the process in the desiccant wheel to the return air;
- the **direct evaporative cooler** is a humidifier, it decreases the air temperature through water vaporisation;
- the **regeneration heat exchanger** that is necessary because the desiccant wheel has to be regenerate to be used continuously and a minimal temperature is necessary for regeneration.

The two other components seen in **Figure 2.1** are ventilation devices necessary to operate the installation. The cycle created by the system is represented on the psychrometric diagram in **Figure 2.2**.

It can be seen that two flows are distinct, from state 1 to 4 and from state 5 to 9, representing the process and the regeneration flow. The different steps are as follows :

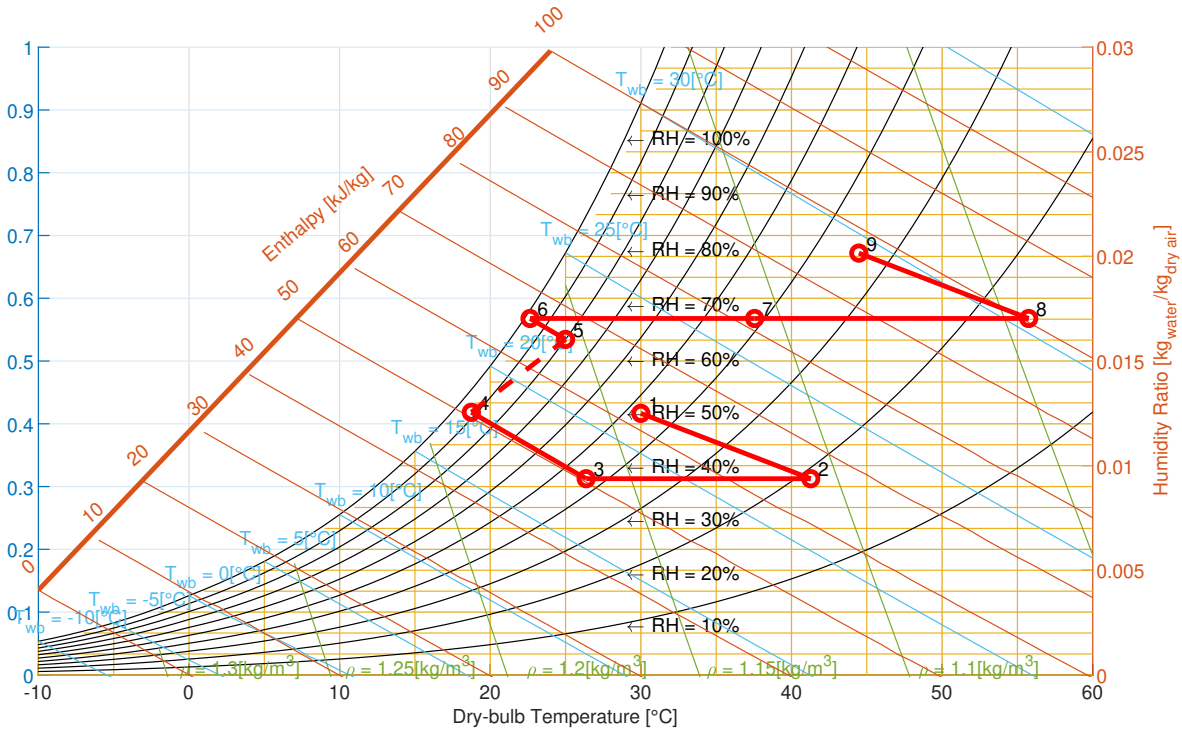

Figure 2.2: Desiccant evaporative cooling system on the psychrometric diagram.

- From state 1 to state 2 : the process air passes through the desiccant wheel so the moisture from the air is absorbed what reduces its humidity and the temperature increases.
- From state 2 to state 3 : the hot and dehumidified air is cooled in the heat exchanger by the air flowing in the regeneration side. The absolute humidity is constant because there is no mass transfer.
- From state 3 to state 4 : the process air passes through the direct evaporative cooler which cools the air and increases its humidity.

- From state 5 to state 6 : the regeneration air is the return room air which passes through a direct evaporative cooler which cools the air and increases its humidity.
- From state 6 to state 7 : the regeneration air captures the heat contained in the process air into the heat exchanger. So there is an increase of temperature and a constant absolute humidity.
- From state 7 to state 8 : the regeneration air passes through the regeneration heat exchanger to increase its temperature and it keeps a constant absolute humidity.
- From state 8 to state 9 : the air through the desiccant wheel to regenerate it and captures the moisture from the wheel. So the absolute humidity contained in the regeneration air increases and the temperature decreases.

The desiccant evaporative cooling system studied in this paper corresponds to a relatively classic and simple configuration. Others more complex configurations are developed in section 3.

Chapter 3

Literature review

Literature review can be separated into four major parts. The first part reports the literature review already published on the subject, the second describes the different possible configurations of the desiccant evaporative cooling system. The third part gathers articles related to the modelling of the different components and the last part reports the performance studies published and the applications of such system around the world.

3.1 Publisher literature review

Previous literature review on the subject have been published. M. Mujahid Rafique et al. [1] developed the background and need of alternative cooling systems, concept of conventional and desiccant evaporative coolers, system configurations, operational modes, as well as current status of the desiccant based evaporative cooling technology. They explained the great potential of desiccant based evaporative cooler of providing human thermal comfort conditions in comparison with conventional cooling systems. They also introduced some modified and modern evaporative coolers.

K. Daou [3] studied the general desiccant cooling air conditioning of which desiccant evaporative cooling belongs. They describe the principles of desiccant cooling and their actual technology applications. Some commented examples are presented to illustrate how the desiccant cooling can be perfect supplement to other cooling systems such as traditional vapour compression air conditioning system, the evaporative cooling, and the chilled-ceiling radiant cooling. It is shown this technology can render evaporative cooling or chilled-ceiling applicable under diverse climatic conditions.

3.2 Different possible configurations

There are different variants of the standard version explained in chapter 2. The standard version is named the ventilation cycle system configuration where the process air is the ambient air that is cooled and injected into the room. The return air is used for the regeneration.

These variants can be separated into two different categories. The first one for changing in the flux configuration and the second for changing/adding components on the initial flux.

3.2.1 Different flux configuration

Several configurations are proposed by M. Ali et al. in their article [4]. These configurations are the following.

A first change on the standard cycle is to reject the return air from the room into the environment and to use the ambient air for regeneration. This configuration is called modified ventilation and have a high dependence on the climatic conditions.

Another change that can be made on the standard version is to use the return air from the room as process air to be injected into the room. The regeneration air uses the ambient air. This configuration is called the recirculation cycle. The main advantage of this cycle is that the system is less dependent on the climate conditions and so have a relatively constant cooling capacity. The major drawback of such a cycle is lack of fresh air provided by the system because it employs 100% recirculation.

In response of this last problem, an evolved configuration is propose, the ventilated-recirculation cycle. In this configuration, the process air is a combination of the recirculation and the ambient air. The amount of ventilation for commercial and institutional buildings is approximately 10-40% of outdoor air.This cycle is represented in the **Figure 3.1**.

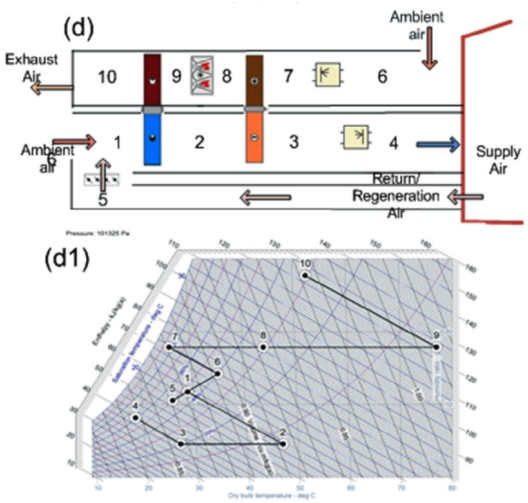

Figure 3.1: Schematic of the ventilated recirculation cycle system configuration [4].

A different proposed configuration is the Dunkle cycle which combines the advantages of ventilation and recirculation cycles. To improve the efficiency, an additional heat exchanger is integrated in the system to benefit of relatively low supply air temperature.This configuration has the same main drawback than the recirculation cycle because the system employs 100% recirculation.

The alternative is the ventilated-dunkle cycle with a combination of ambient air and recirculation. This cycle is less efficient because it uses ambient air but it is necessary to have a sufficient air quality for sanitary reasons. This cycle is represented in the **Figure 3.2**.

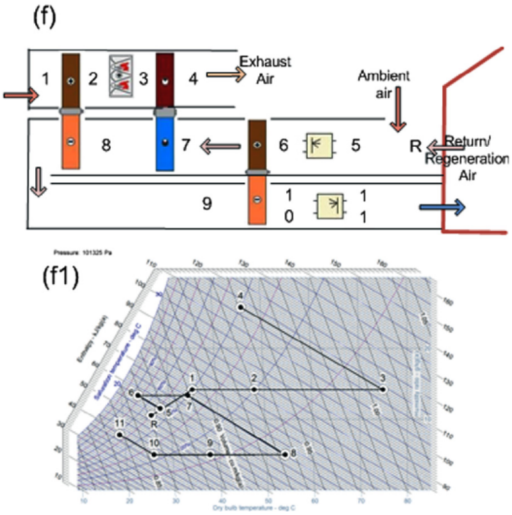

Figure 3.2: Scheme of the ventilated Dunkle cycle system configuration [4].

3.2.2 Alternative to direct evaporative cooling for standard cycle

Direct/indirect evaporative cooler

E. Elgendy et al. proposed the use of a direct/indirect evaporative cooler in the cycle [5]. An indirect evaporative cooler is a heat exchanger in which the secondary fluid is humidified. Its temperature is hence decreased and the flux can be used to sensibly cool the primary air.

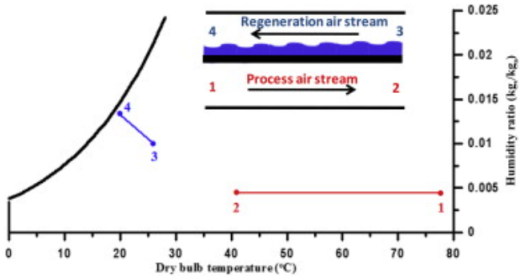

Figure 3.3: Process of direct/indirect evaporative cooler on psychrometric diagram [5].

A first configuration is the use of a direct/indirect evaporative cooler instead of the direct evaporative cooler in the regeneration side. The DIEC is added just before the heat exchanger in the process air side.

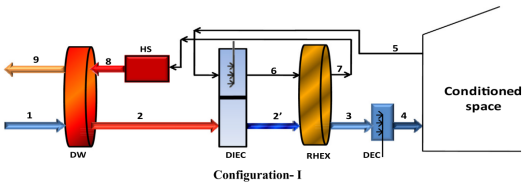

Figure 3.4: Desiccant evaporative cooling system configuration-I [5].

The second variant is to place the DIEC after the heat exchanger and before the direct evaporative cooler.

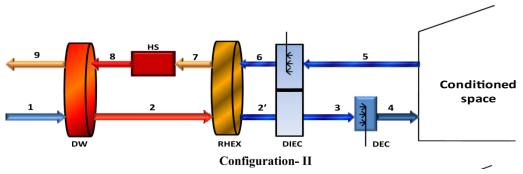

Figure 3.5: Desiccant evaporative cooling system configuration-II [5].

Finally the last proposed configuration is the addition of a second DIEC between the DIEC-I and the direct evaporative cooler but such that it is the process air that is humidified.

E. Elgendy et al. [5] realised the simulation and the comparison between these three novel desiccant evaporative cooling system configurations with the conventional system under a wide range of ambient temperature and humidity ratio. Validation results confirm that, simulation and experimental results are in a good agreement. Energetic analysis revealed that configuration-I has the highest cooling capacity while configuration-III has the highest thermal COP and air handling COP.

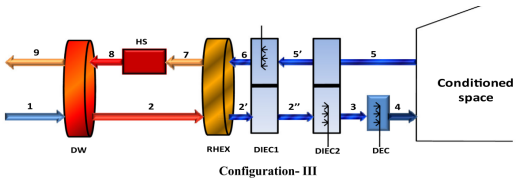

Figure 3.6: Desiccant evaporative cooling system configuration-III [5].

Wet-surface heat exchanger

An alternative to the classical heat exchanger is the wet-surface heat exchanger (WSHE) in which the air can be cooled to its dew-point temperature. This new component leads to new configurations as developped by S. Jain et al. [6]. In a wet-surface heat exchanger, the incoming process air is indirectly cooled by water. The water is in turn cooled by recirculated part of the process air. The ratio of the recirculated air to the total incoming air, called the extraction, is assumed to 50%.

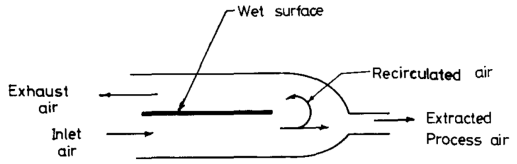

Figure 3.7: Schematic of a Wet-surface heat exchanger [6].

S. Jain et al. [6] investigated the effectiveness of heat exchangers/evaporative coolers on the cooling coefficient of performance and volumetric air flowrate per unit cooling capacity. Different configurations were studied, ventilation, recirculation, 10% ventilated recirculation, dunkle, 10% ventilated dunkle and four cycles with WSHE. The conclusion was that cycles using wet surface heat exchangers give even higher performance.

Dew-point indirect evaporative cooler

An alternative to the direct evaporative cooler is the dew-point indirect evaporative cooler (DPIEC). It consists in a three-stage heat exchanger in which the process air is cooled by a working air. The process can be seen on **Figure 3.8**. The main advantage of such technology is that the output temperature in the dry channel is lower than with a classical indirect evaporative cooler.

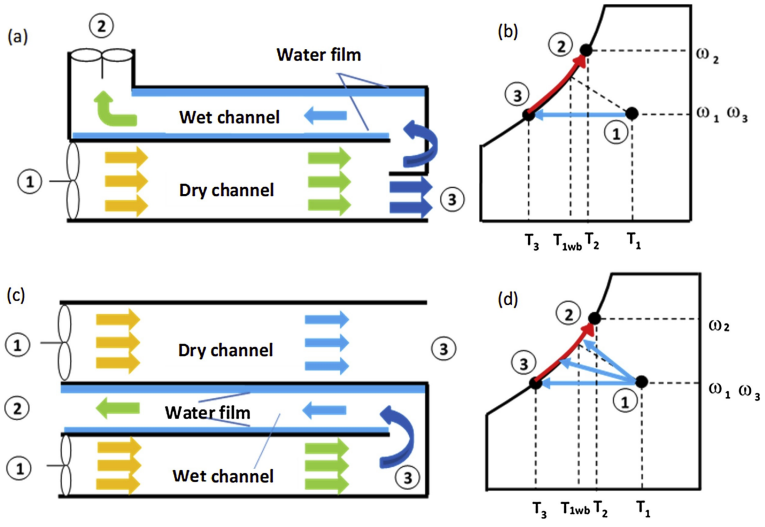

Figure 3.8: Dew-point indirect evaporative cooler

It can be noticed that the dew-point temperature can be reached only for an ideal case because in

practice this temperature cannot be reached.

Y.E. Güzelel et al. [7] investigated a desiccant based air-conditioning system supported by a dew-point indirect evaporative cooler. A mathematical model of the air-conditioning system was developed by deriving new equations for modelling two key components of the system, namely desiccant wheel and dew-point indirect evaporative cooler using the available correlations and experimental data. A validation of the modelling is performed.

Maisotsenko cycle

The Maisotsenko cycle that is applied in air-conditioning as presented by L. Lai et al. in their article [8] as well as G.Q. Chaudhary et al. in their article [9] is an evolution of the dew-point indirect evaporative cooler. The Maisotsenko cycle is represented on **Figure 3.9**.

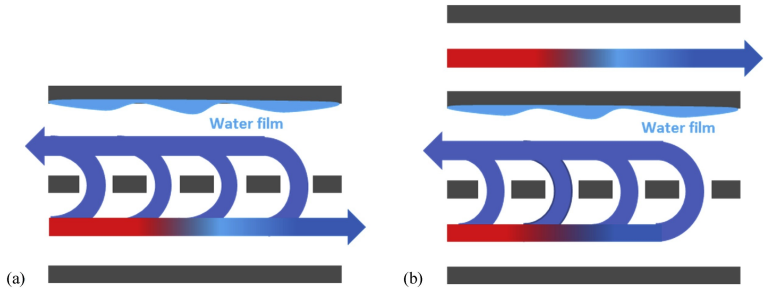

Figure 3.9: Maisotsenko cycle

It can be seen that some air from the lowest channel passes through small openings. This technology brings best efficiency than the DPIEC.

L. Lai et al. [8] evaluated a solar-assisted solid desiccant Maisotsenko cycle based indirect evaporative cooling system with different recirculation air ratios. Three other cooling systems, including stand-alone direct evaporative cooling, stand-alone Maisotsenko cycle based indirect evaporative cooling, and conventional solid desiccant evaporative cooling system were simulated and compared with the proposed system under various ambient conditions. The solar-assisted solid desiccant Maisotsenko cycle based indirect evaporative cooling system had the best cooling performance compared with the other three systems.

G.Q. Chaudhary et al. [9] investigated an integrated solar assisted cooling system consisting of a solid desiccant system for handling latent load and a Maisotsenko cycle based evaporative cooling system for sensible load. The experimental setup consists of a purposely designed hybrid arrays of solar thermal collectors, a solid desiccant wheel with heat recovery and a coupled indirect Maisotsenko evaporative cooler in cross flow arrangement. The dehumidification effectiveness, dew point effectiveness, thermal COP, and cooling capacity are tested for the integrated system.

Two-stage evaporative cooler

In two-stage evaporative cooling both direct and indirect process are combined. Firstly, an indirect evaporative cooling occurs, after a damper directs the flow to a direct evaporative cooler or a by-pass channel to finally mix the two flows. This technology and these modern evolution are developed by M. Mujahid Rafique et al. [1].

Wet membrane humidifier

A wet membrane humidifier is used as alternative to the direct evaporative cooler. The core of a wet membrane humidifier is a wet film materials composed of polymers composites. Under the effect of gravity, water sent to the top of the humidifier percolates down along the surface of the wet membrane

to form an even water membrane on the surface of the wet membrane and then cools and humidifies the hot and dry air. L.Chen et al. [10] built an experimental setup and tested the performances of three modes for dedicated desiccant wheel outdoor air cooling systems.

3.3 Modelling of the components

All the component of the desiccant evaporative cooling system have to be model. These elements are the desiccant wheel, the direct evaporative cooler and the heat exchanger. The literature corresponding to these components are compartmentalised in corresponding sections.

3.3.1 Desiccant wheel

D.B. Jani et al. [11] developed a rigorous literature review in which, different configurations of desiccant cooling cycles, conventional and hybrid desiccant cooling cycles, different types of mathematical models of rotary desiccant dehumidifier, performance evaluation of desiccant cooling system, technological improvement and the advantage it can offer in terms of energy and cost savings are highlighted. The most interesting element developed are the different types of mathematical models of rotary desiccant dehumidifier.

S. Yamaguchi et al. [12] focus on a rotary desiccant wheel which is the main component of the desiccant air-conditioning system and develop and validate the mathematical model by comparison with experimental results. The mathematical model is very complete and goes into great detail.

G. Panaras et al. [13] performed a study which is an experimental validation of a simplified approach for a desiccant wheel model, based on the concept of the analogy method and the formulation for the respective combined potentials. The validation is investigated experimentally.

F.E. Nia et al. [14] realised the modelling of a desiccant wheel used for dehumidifying the ventilation air of air-conditioning system. The model is validated through comparison the simulated results with the published actual values of an experimental work. The modelling solutions are used to develop simple correlations for the outlet air conditions of humidity and temperature of air through the wheel as a function of the physically measurable input variables.

3.3.2 Direct evaporative cooler

A. Fouda et al. [15] developed a simplified mathematical model to describe the heat an mass transfer between air and water in a direct evaporative cooler. The study presents a comparison of the computed results with that of experimental results for the same evaporative cooler. A good agreement between the calculated and experimental results is achieved.

3.4 Performance studies and applications

Some articles are a complete performance analysis of a desiccant evaporative cooling system applied to a specific climate. These articles are gathered below.

M. Mujahid Rafique et al. [16] developed a mathematical model of the desiccant evaporative cooling and analysed the performance of the system for its feasibility under the climatic conditions of city in Saudi Arabia. The results showed that the proposed system is suitable and feasible solution to meet the high cooling demands for the conditions of Saudi Arabia with performance largely dependent on optimum selection of operating parameters.

Y. Ma et al. [17] studied the system performance of a solar desiccant evaporative cooling system with a reference conventional variable air volume system in Australia. A simulation model of the building is developed with EnergyPlus. The performance indicators for the comparison are system

coefficient of performance, annual primary energy consumption, annual energy savings and annual CO_2 emissions reduction. The results show that Darwin cycle is the most efficient.

L. Merabti et al. [18] studied an desiccant evaporative cooling system coupled with a solar installation. The results show that the system can control moisture and therefore provide acceptable comfort conditions.

M. Ali et al. [4] performed an investigation on the optimal configuration of desiccant evaporative cooling systems for specific climatic zones. In this study, five cities corresponding to five different zones in the world were chosen. Five system configurations were studied : ventilation, recirculation, ventilated-recirculation, dunkle and ventilated-dunkle cycles. The optimal configurations are determined for each climate zone using an advance equation-based object-oriented modelling and simulation approach. The performance parameters selected for the comparison are cooling capacity, COP and cooling energy delivery. The results revealed that ventilated-dunkle and ventilation cycle are the most efficient depending on the climatic zone.

3.5 Conclusion

In this section it can be noticed that several articles have been published the on desiccant evaporative cooling system. Some papers report the different possible configurations or others design propositions. Complete modelling of the component, in particular the desiccant wheel is realised. Some articles relate to the performance and the possible application of such technology.

Chapter 4

Modelling and validation

In this section the modelling of the desiccant evaporative cooling system is carried out. Firstly, the modelling of the building is discussed with a brief description of the building, the parameter selection as well as the weather data. The internal temperature of the building and the HVAC load over the year is given as result of the building model.

Secondly, the modelling of the cycle is performed with the general resolution of the cycle by a description of the iterative scheme. All the components of the cycle are described and modelled. A parametric analysis is realised for each model. For the desiccant wheel and the rotary air to air heat exchanger, a simple and a complex model are provided. A calibration of these simple models is realised from data generated by the complex model as well as a validation to determine the relevance of such calibration.

4.1 Modelling of the cooling load of the building

The building is modelled in order to determine the heating and the cooling loads as well as the internal temperature of the building. Only the cooling load is necessary for the desiccant evaporative cooling system model. In this section, a brief description of the building is given as well as the parameters used in the modelling. The model provided by A. Zeoli is succinctly described and finally the results are represented to be used in the modelling of the cooling system.

4.1.1 Description of the building

The building in which the desiccant evaporative cooling system is installed is a large office building suffering from chronic overheating in the summer and intermediate seasons. This test building is a university building comprising student rooms, teaching rooms, office rooms, meeting rooms and dining hall. The university building is located in Aalborg in Denmark and named CREATE. The building is represented on **Figure 4.1**.

Figure 4.1: View of the building study case : CREATE - Rendsburggade 14, 9000 Aalborg, Denmark [2]

The CREATE building is located in the Aalborg city centre next to a fjord. The location of the CREATE building in its surrounding environment can be seen on **Figure 4.2**.

Figure 4.2: Aerial view of the CREATE building in its surrounding environment in Aalborg city center [2]

The desiccant evaporative cooling system is used in one of the six different zones of the building. The building is divided into six zones with independent energy management. In the present study, only the considered zone is modelled. This zone is located in the south east of the building.This zone is composed of 3 floors.

4.1.2 Selection of parameters and weather data

The usage schedule of the building is the schedule proposed for a school or a classroom from the *ISO/TC163WG4* [19]. The schedule is given in the **Table 4.1**.

h	Occupants/ Appliances/ Lighting		h	Occupants/ Appliances/ Lighting
1	0		13	**0.3**
2	0		14	**0.7**
3	0		15	**0.6**
4	0		16	**0.4**
5	0		17	**0.2**
6	0		18	0
7	0		19	0
8	0		20	0
9	**0.6**		21	0
10	**0.7**		22	0
11	**0.6**		23	0
12	**0.4**		24	0

Table 4.1: Usage schedule of the room for energy calculation

The corresponding parameters for occupants, appliances and lighting is deduced from a combination configuration. The building is a combination of student rooms, teaching rooms, office rooms, meeting rooms and dining rooms so the parameters of these configurations are gathered in **Table 4.2**.

Configuration	Occupants $[W/m^2]$	Appliances $[W/m^2]$	Lighting $[W/m^2]$
School / classroom	21.7	8	/
Meeting room	59.2	12	/
Office single	11.8	12	/
Restaurant	19.4	4	/
CREATE building	**50**	**8**	**1**

Table 4.2: Building parameters determination from the *ISO/TC163WG4* standards.

The CREATE building parameters are determined from the different configurations possible with a high level of occupancy. This is due to the fact that real occupancy of the CREATE building is significantly higher than what was estimated during the design phase as explained by Johra [2].

The nominal ventilation of the zone is equivalent to $15000[m^3/h]$. It is the nominal airflow rate of the desiccant evaporative cooling system installed in the CREATE building. For the modelling, the ventilation rate for each sub-zone is proportional to the volume of this sub-zone or the following equation 4.1.

$$\text{ventilation rate of a sub-zone} = \text{nominal ventilation rate} \times \frac{\text{Volume of the sub-zone}}{\text{Total volume of the zone}} \tag{4.1}$$

This ventilation rate applies to both the air supply and exhaust. The infiltration is supposed to be equal to $0.2ach$.

Some set-point temperatures are fixed into the model to start cooling, heating or window opening. When the internal temperature is lower than $22°C$, the heating starts. When the temperature is higher than $24°C$, the cooling starts. The window opening occurs when the internal temperature exceeds $23°C$. The cooling and the heating load are limited to a maximum value for each sub zone depending on the volume of the zone as for the ventilation rate taking into account the proportion of

the sub-zone into the total. The sum of all the loads leads to the total heating/cooling load that is $78kW$.

The weather data of Aalborg come from the European platform *PVGIS* which contains the meteorological data for Europe. The file use in this study is the *Typical Meteorological Year* for the geographical coordinates of the building : (57.048, 9.930). The TMY file contains several information such as air temperature [$°C$], relative humidity [%], global irradiance on the horizontal plane [W/m^2], Beam/direct irradiance on a plane always normal to sun rays [W/m^2], Diffuse irradiance on the horizontal plane [W/m^2], Surface infrared (thermal) irradiance on a horizontal plane [W/m^2], total wind speed [m/s] and wind direction [°].

The external temperature nearby the building is represented on the **Figure 4.3**.

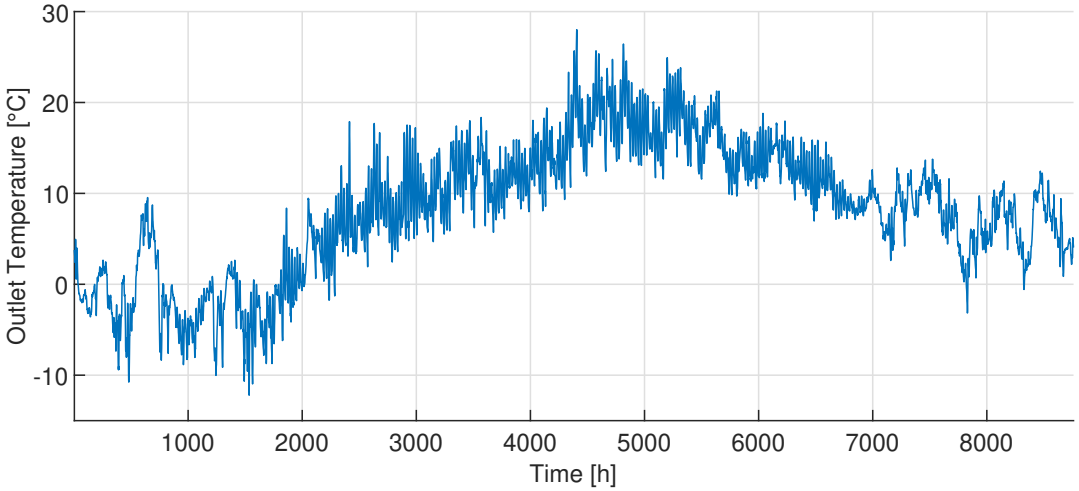

Figure 4.3: External temperature nearby the building in Aalborg from the *PVGIS* plateform.

It can be seen that the external temperature is relatively low and does not frequently exceeds $20°C$. But in the situation of climate change with important periods of overheating during summer, these outlet temperatures would probably increase.

The external relative humidity is represented on **Figure 4.4**.

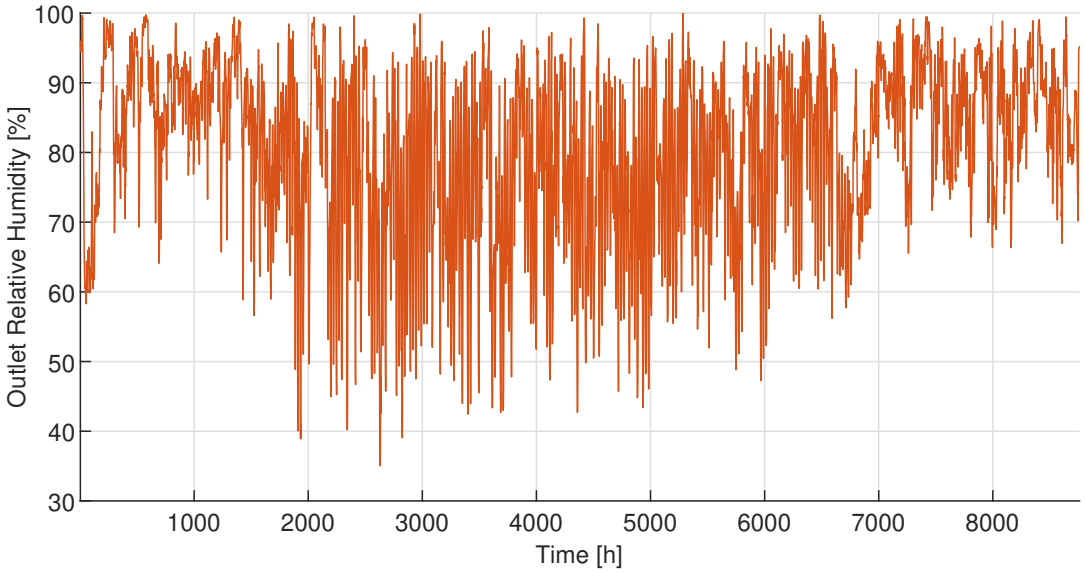

Figure 4.4: External relative humidity nearby the building in Aalborg from the *PVGIS* plateform.

The relative humidity of this region, close to a fjord is relatively high throughout the year. The relative humidity is particularly high during winter and has greater fluctuation during the summer.

4.1.3 Modelling

The building model provided by Zeoli is based on heat transfer through walls and windows. This model resolves the thermal balance in the building for all hours of the year, depending on the weather conditions, the configuration of the building (geometry and envelope properties), the operation intake and the ventilation and HVAC constraints. The model takes into account the dynamic effects of the building as the inertia of the building. The conditions at time t requires to know conditions at time $t-1$.

The results of the model are the internal temperature in each sub-zone of the building and the heating/cooling load per sub-zone. The building generally needs heating during winter, cooling during summer and a combination of both during the intermediate seasons.

4.1.4 Results

The results of the modelling provided by Zeoli are the internal temperature and the heating/cooling load for each sub-zone of the building. The cooling/heating load is positive when the system is in heating load and negative for the cooling load. In order to have a simpler expression of the temperature, the mean of the temperature of each room is calculated. This mean internal temperature is represented on **Figure 4.5**.

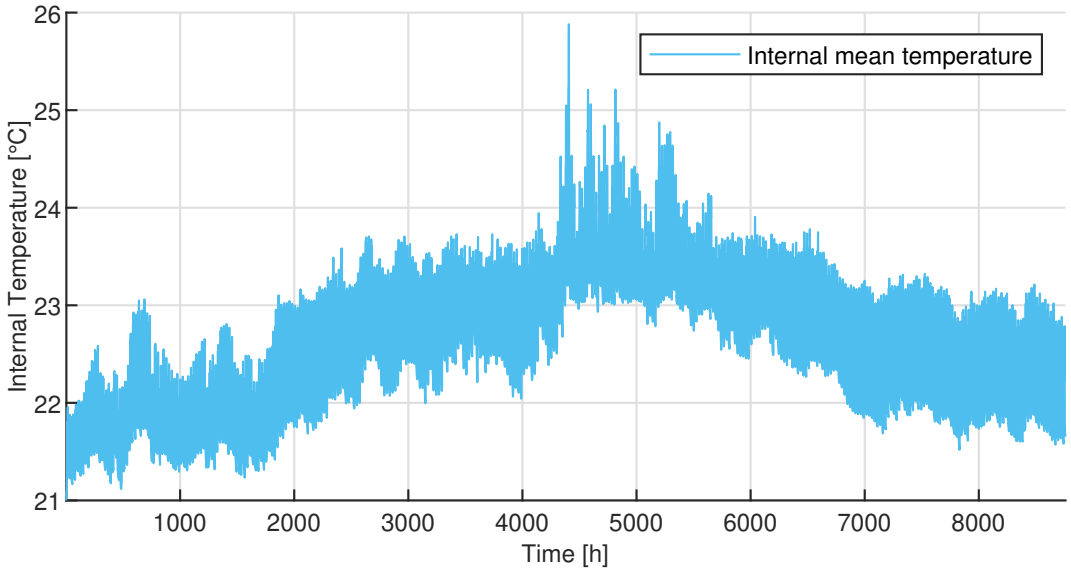

Figure 4.5: Mean internal temperature in the zone of the building over the year.

It can be seen that the mean internal temperature generated by the building model is relatively constant and oscillates from 21 to 24°C with pics until 26°C. Generally, the temperature is included between 22 and 24°C that are the set-point temperature for heating and cooling. When the temperature exceeds these boundaries, it means that the cooling or the heating load is at is maximal level.

Concerning the HVAC load, the sum of the cooling and heating load is carried out in order to have the total energy injected into the room. The HVAC load is represented on **Figure 4.6**.

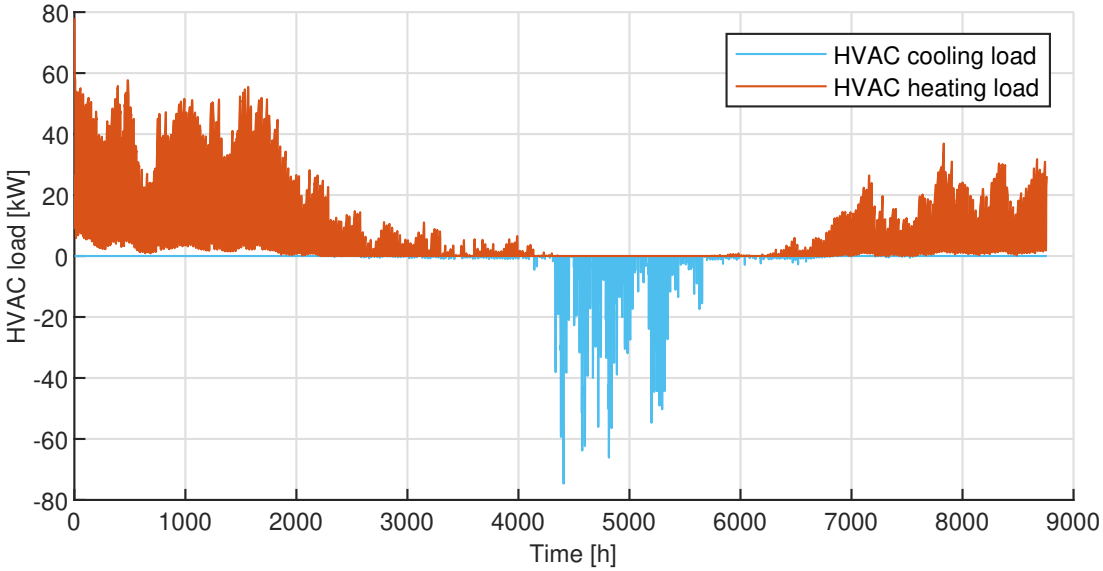

Figure 4.6: HVAC result power load in heating and cooling mode.

It can be noticed that the heating load is represented in orange on the graphic while the cooling load is represented in blue. From the building model, the need for cooling is highly focused on summer. During intermediate seasons, there is cooling load of low amplitude.

4.2 Modelling of the cycle

The cycle can be modelled by a general loop using functions for each component. This leads to evaluate the impact of the level of complexity of the model.

Firstly, the iterative scheme of the cycle is given gathering all the components.

In a second step, all the components of the cycle are described. A simple model for each component is realised. For the desiccant wheel and the rotary air to air heat exchanger, a complex modelling is performed. All the models are analysed with a parametric study to evaluate the impact of these parameters on the output of these models. From the complex model, a data set is generated in order to calibrate the simple model on the complex one. These calibrations are then validated to evaluate the calibration level.

4.2.1 Iterative scheme

The iterative scheme of the complete model in provided in **Figure 4.7**.

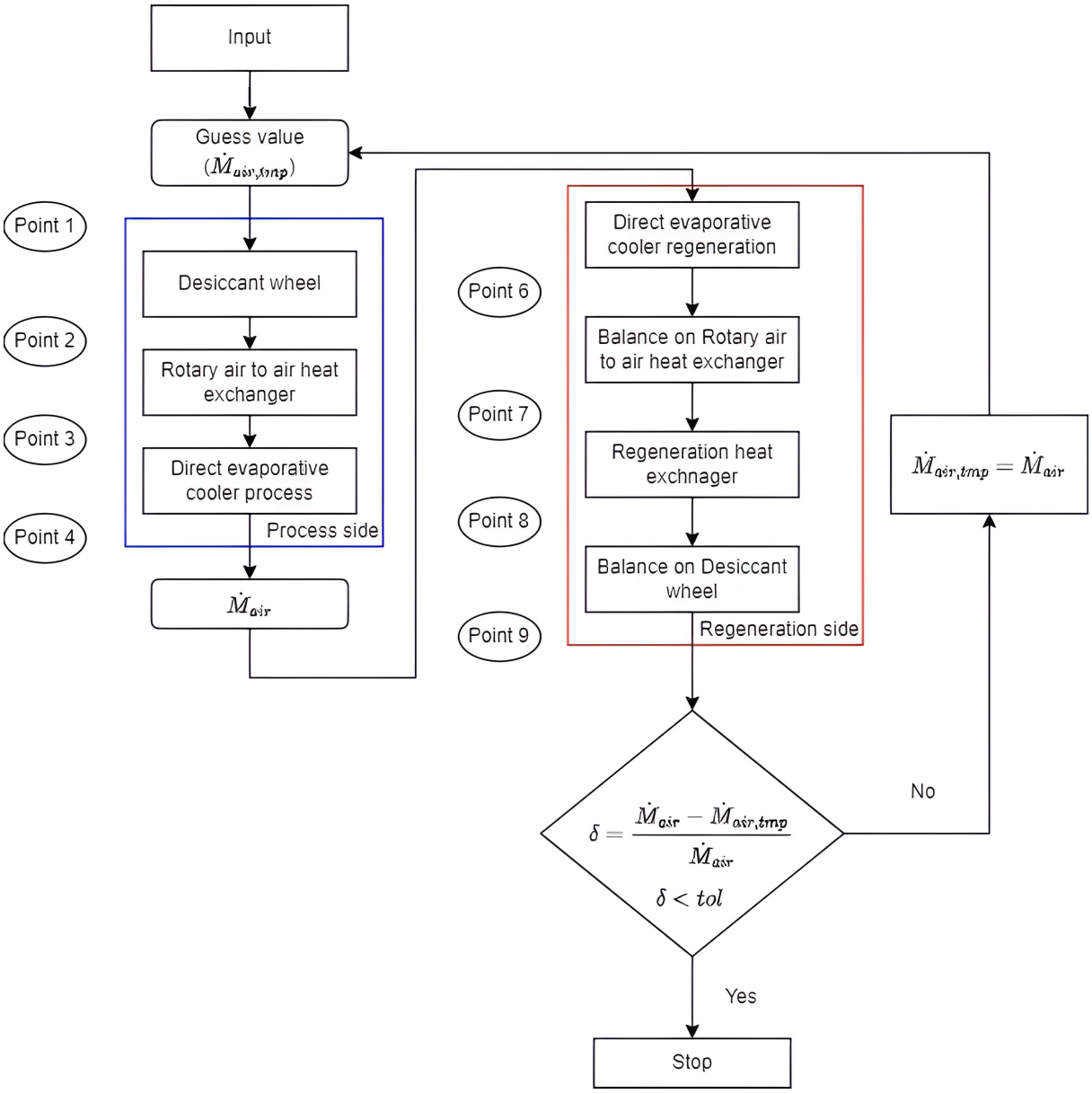

Figure 4.7: Iterative scheme of the complete model.

As a reminder, the scheme of the desiccant evaporative cooling system is represented in **Figure 4.8** to help understand the cycle.

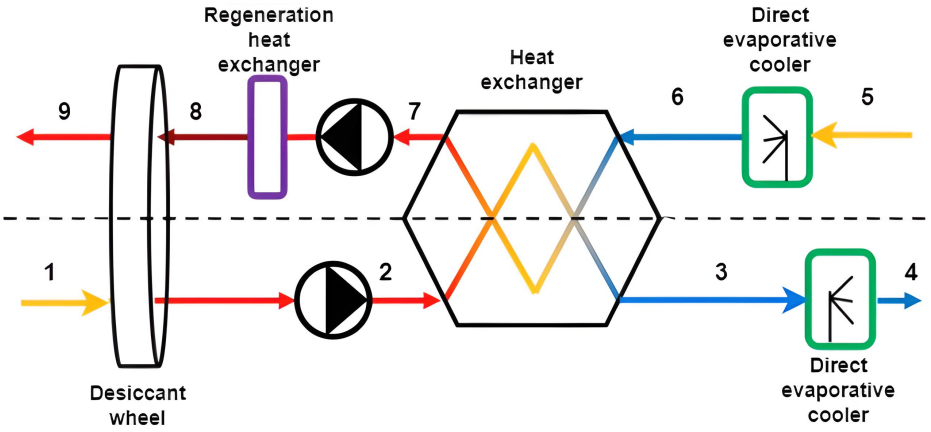

Figure 4.8: Desiccant evaporative cooling system scheme [2].

At the beginning, all state points are initialised to allow to use the different models related to the components of the cycle. For example, it is necessary to know the state conditions 1 and 9 to use the desiccant wheel model.

The air mass flow rate $\dot{m}_{air}$ is firstly fixed at a nominal mass flow rate computed from the nominal airflow rate provided by H. Johra [2] equivalent to $\dot{V}_{air} = 15000 m^3/h$. In the model, the air mass flow rate is corrected by making an energy balance on the room, equation 4.2:

$$Q_{room} = \dot{m}_{air} \times (h_5 - h_4) \Leftrightarrow \dot{m}_{air} = \frac{Q_{room}}{h_5 - h_4} \tag{4.2}$$

where Q_{room} is the ventilation power representing the power discharged from the room, h_5 is the enthalpy of the air coming out of the room which is fixed by the building model and h_4 the enthalpy of the air entering the room.

A balance on the rotary air to air heat exchanger is necessary to determine the exhaust air on the regeneration side. It is only a question of an energy balance as there is no mass transfer into the exchanger. The balance is the following :

$$Q_{HRW,pro} = -Q_{HRW,reg} \Leftrightarrow \dot{m}_{air} c_{p,air} \times (T_3 - T_2) = -\dot{m}_{air} c_{p,air} \times (T_7 - T_6) \tag{4.3}$$

Since the air mass flow rate is equivalent in the regeneration and in the process side as well as there is no important variation in specific heat, the equation becomes :

$$T_3 - T_2 = T_6 - T_7 \Leftrightarrow T_7 = T_6 - (T_3 - T_2) \tag{4.4}$$

Similarly for the desiccant wheel, balances lead to determine the output conditions on the regeneration side. In this case, an energy balance as well as a mass balance are necessary as described by Rafique et al. [16]. The energy balance with a similar reasoning as for the air to air rotary heat exchanger brings :

$$T_9 = T_8 - (T_2 - T_1) \tag{4.5}$$

The mass balance is the following :

$$\dot{m}_{water,pro} = -\dot{m}_{water,reg} \Leftrightarrow \dot{m}_{air,pro} \times (w_2 - w_1) = -\dot{m}_{air,reg} \times (w_9 - w_8) \tag{4.6}$$

$$w_2 - w_1 = w_8 - w_9 \Leftrightarrow w_9 = w_8 - (w_2 - w_1) \tag{4.7}$$

The iterative loop corrects the air mass flow rate until the system converges.

4.2.2 Desiccant wheel

The desiccant wheel is used to dehumidify the process air from the outside in order to cool it and to inject it into the room as represented on **Figure 4.9**. The desiccant wheel contains adsorbent which is able to capture moisture from the air and to be regenerated by a warm and dry air.

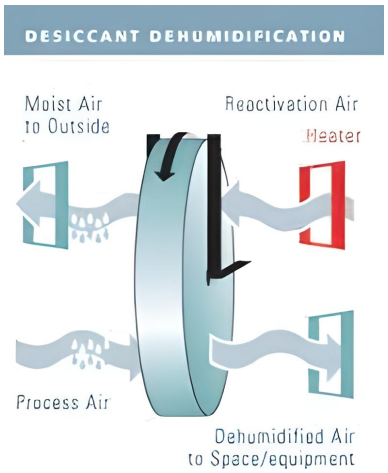

Figure 4.9: Desiccant wheel representation [20].

The dehumidification is a process of combined heat and mass transfer between the air and the desiccant material.

In this section, a simple model of the desiccant wheel is investigated followed by the complex model including the heat and mass transfer equations. Finally, the calibration and the validation of the simple model is performed from the data generated by the complex model.

Simple model

The simple model proposed by Panaras et al. [13] gives empirical relations on the basis of experimental data.

The model proposed can be described by the following equations (4.8), (4.9), (4.10) and (4.11) with $i = 1, 2$ and 8 :

$$F_{1,i} = \frac{-2865}{(T_i + 273.15)^{1.49}} + 4.344(w_i)^{0.8624} \tag{4.8}$$

$$F_{2,i} = \frac{(T_i + 273.15)^{1.49}}{6360} - 1.127(w_i)^{0.07969} \tag{4.9}$$

$$\eta_{F1} = \frac{F_{1,2} - F_{1,1}}{F_{1,8} - F_{1,1}} \tag{4.10}$$

$$\eta_{F2} = \frac{F_{2,2} - F_{2,1}}{F_{2,8} - F_{2,1}} \tag{4.11}$$

States at the inlet of the desiccant wheel on the process side (position 1 on **Figure** 2.2) and at the inlet on the regeneration side (position 8) are known. So temperature and absolute humidity can be used to determine the values of characteristic potentials $F_{1,1}$ and $F_{1,8}$ from equation (4.8) and $F_{2,1}$ and $F_{2,8}$ from equation (4.9). From given values for efficiency factors η_{F1} and η_{F2}, $F_{1,2}$ and $F_{2,2}$ can be determined from equations (4.10) and (4.11). Finally, the corresponding outlet temperature and absolute humidity on the process side can be determined.

The value of the efficiency factors are determined experimentally in different articles. Below a table gathering these different values.

η_{F1}	η_{F2}	Article
0.15	0.69	[13]
0.05	0.95	[8]
0.05	0.95	[21]

Table 4.3: Efficiency factor determination in corresponding studies.

As expressed by Panaras et al. [13], the typical examples of fixed, preset values can be found as follows :

- $(\eta_{F1}, \eta_{F2}) = (0.05, 0.95)$: high performance wheel;
- $(\eta_{F1}, \eta_{F2}) = (0.08, 0.8)$: moderate performance wheel;
- $(\eta_{F1}, \eta_{F2}) = (0.1, 0.7)$ or $(\eta_{F1}, \eta_{F2}) = (0.07, 0.8)$: low performance wheel.

Parametric study

A parametric study on the two parameters η_{F1} and η_{F2} leads to evaluate the impact of the parameter value on the output values, the output temperature T_2 and the output specific humidity w_2 on the process side.

For this purpose, an analysis for each parameter is performed. One parameter is kept constant while the other evolves.

Firstly, **Figure 4.10** represents the evolution of output temperature and specific humidity when η_{F1} variate between 0 and 0.5 while $\eta_{F2} = 0.8$.

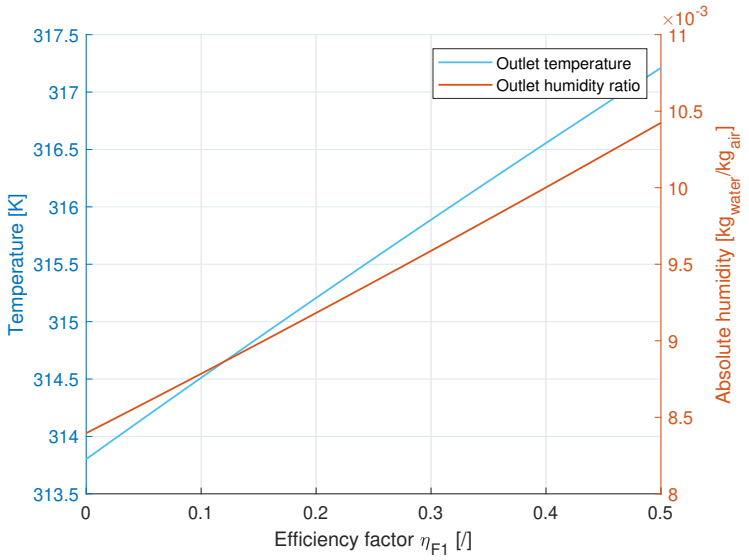

Figure 4.10: Parametric study of the desiccant wheel model when η_{F1} evolves.

It can be seen that both, temperature and specific humidity increase when the parameter η_{F1} increases. The best desiccant wheel would have $\eta_{F1} = 0$ as the objective is to remove moisture from the air while keeping the temperature as low as possible at the wheel outlet.

In the second case, the parameter η_{F2} evolve between 0 and 1 while $\eta_{F1} = 0.08$. The **Figure 4.11** is represented just below :

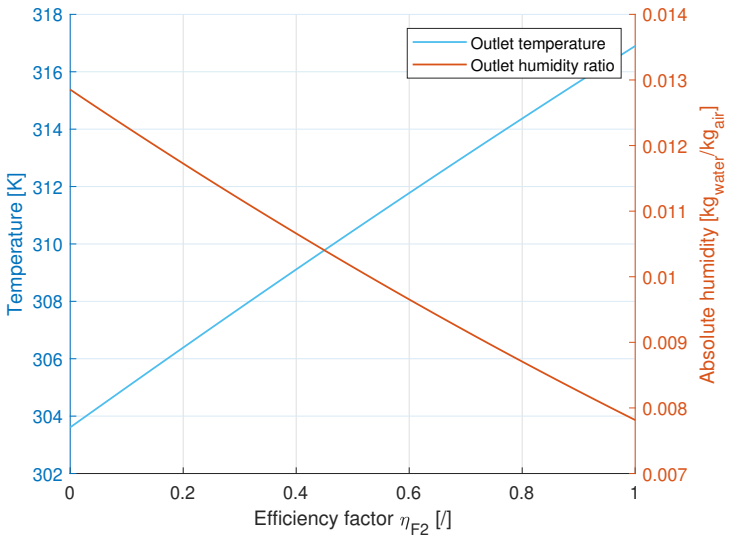

Figure 4.11: Parametric study of the desiccant wheel model when η_{F2} evolves.

It can be noticed that the outlet temperature increases while the outlet specific humidity decreases when the parameter η_{F2} increases. The very first objective of the desiccant wheel is to remove the moisture from the ambient air so the best parameter η_{F2} is the highest which gives a lowest absolute humidity.

Complex model

The complex model in based on heat and mass exchanger. The exchanger is design with the effectiveness - NTU method including a corrective factor taking into account the rotation speed of the wheel developed by Wrobel et al. [22].

Firstly, an adsorption equilibrium of fluid at each inlet of the desiccant wheel respectively on the process and the regeneration side named $i = 1, 8$. This balance is done for the calculation of water load $q_{i,in}$ at adsorbent. The correlation used in the paper needs to determine firstly the factors $a_{i,in}$ and $b_{i,in}$ from the inlet temperature $T_{i,in}$.

$$a_{i,in} = -4 \times 10^{-3} \times (T_{i,in} - 273.15) + 2.2204 \tag{4.12}$$

$$b_{i,in} = 4.6 \times 10^{-3} \times (T_{i,in} - 273.15) - 1.5071 \tag{4.13}$$

these factors are used in the equilibrium equation

$$\varphi_{i,in} = \exp\left[-\left(\frac{q_{i,in}}{a_{i,in}}\right)^{b_{i,in}} \right] \tag{4.14}$$

with $\varphi_{i,in}$ the relative humidity of fluid at inlet 1 and 8, state points on the system schema 2.1.

The second step of the model is to determine the efficiencies for enthalpy η_h and the water load η_q. The initial efficiencies are :

$$\eta_{h,0} = 0.15 \tag{4.15}$$

$$\eta_{q,0} = \left(1 - \frac{1}{2.32705 \times |q_{1,in,calc} - q_{2,in,calc}| + 3.99782}\right) + q_{1,in,calc} \times 0.00056222 \tag{4.16}$$

with the terms $q_{1,in,calc}$ and $q_{2,in,calc}$ determine in other to fix the limits such as

$$q_{1,in,calc} = min(10, q_{1,in}) \tag{4.17}$$

$$q_{2,in,calc} = min(8, q_{2,in}) \tag{4.18}$$

The final efficiencies η_h and η_q are determined from the rotation speed of the wheel. The model have been designed on a conventional desiccant wheel with a nominal rotation speed, the parameter $n0$ and the efficiencies of the system are corrected using the real rotation speed variable $rotSpeed\_in$. An iterative scheme illustrated on **Figure 4.12** represents the decision path to determine η_h and η_q.

The general solution, excluding special cases with zero rotation speed and a rotation speed equivalent to the rotation speed parameter $n0$, is determine by equation 4.19 and 4.20 taking the absolute value of the rotation speed $rotSpeed\_in$ when this one is negative.

$$\eta_h = max(min(eta\_h\_rotation(eta_{h1}, n0, rotSpeed\_in), 1), 0) \tag{4.19}$$

$$\eta_q = max(min(eta\_q\_rotation(eta_{h1}, n0, rotSpeed\_in), 1), 0) \tag{4.20}$$

where $eta\_h\_rotation$ and $eta\_q\_rotation$ are correlations used to correct the effectiveness.

The first correlation $eta\_h\_rotation$ take into account the influence of rotation speed on η_h. The equations of this correlation are the following ones :

$$a = 0.1354 \times \eta_{h1} + 0.6386 \tag{4.21}$$

$$\eta_h = \eta_{h1} \times \left(\frac{n}{n0}\right)^a \tag{4.22}$$

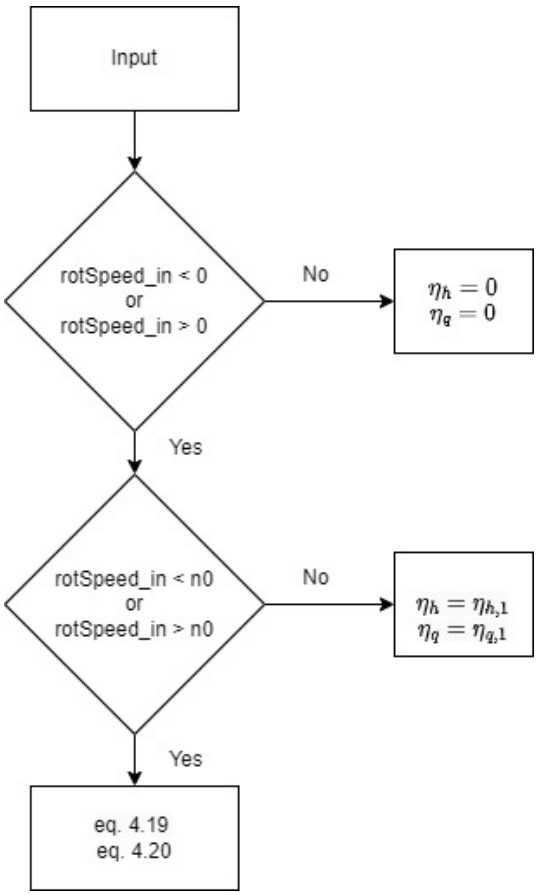

Figure 4.12: Iterative scheme of the complex model of the desiccant wheel for the dependence on rotation speed of the wheel.

The second correlation *eta_q_rotation* is a bit different with several corrective factors :

$$a = 0.6325 \times \eta_{q1}^2 - 1.4986 \times \eta_{q1} + 0.8641 \tag{4.23}$$

$$b = 2.6113 \times \eta_{q1}^{46.0408} + 1.0386 \tag{4.24}$$

$$c = -0.641 \times \eta_{q1}^2 + 0.5151 \times \eta_{q1} + 0.1286 \tag{4.25}$$

$$eta_q = 1 - \left(a \times \left(\frac{n}{n0} \right)^{-b} + c \right) \tag{4.26}$$

From this it is possible to determine the specific enthalpy and the water load at the outlet on the process side.

$$h_{1,out} = h_{1,in} - \eta_h \times (h_{1,in} - h_{2,in}) \tag{4.27}$$

$$q_{1,out} = q_{1,in,calc} - \eta_q \times (q_{1,in,calc} - q_{2,in,calc}) \tag{4.28}$$

In an iterative loop it this possible to determine the temperature and the relative humidity of the fluid in the process side at outlet depending on $h_{1,out}$ and $q_{1,out}$. This iterative loop is represented on **Figure 4.13**.

Finally from enthalpy and relative humidity it brings the absolute humidity $w_{1,out}$ at the outlet of the desiccant wheel on the process side.

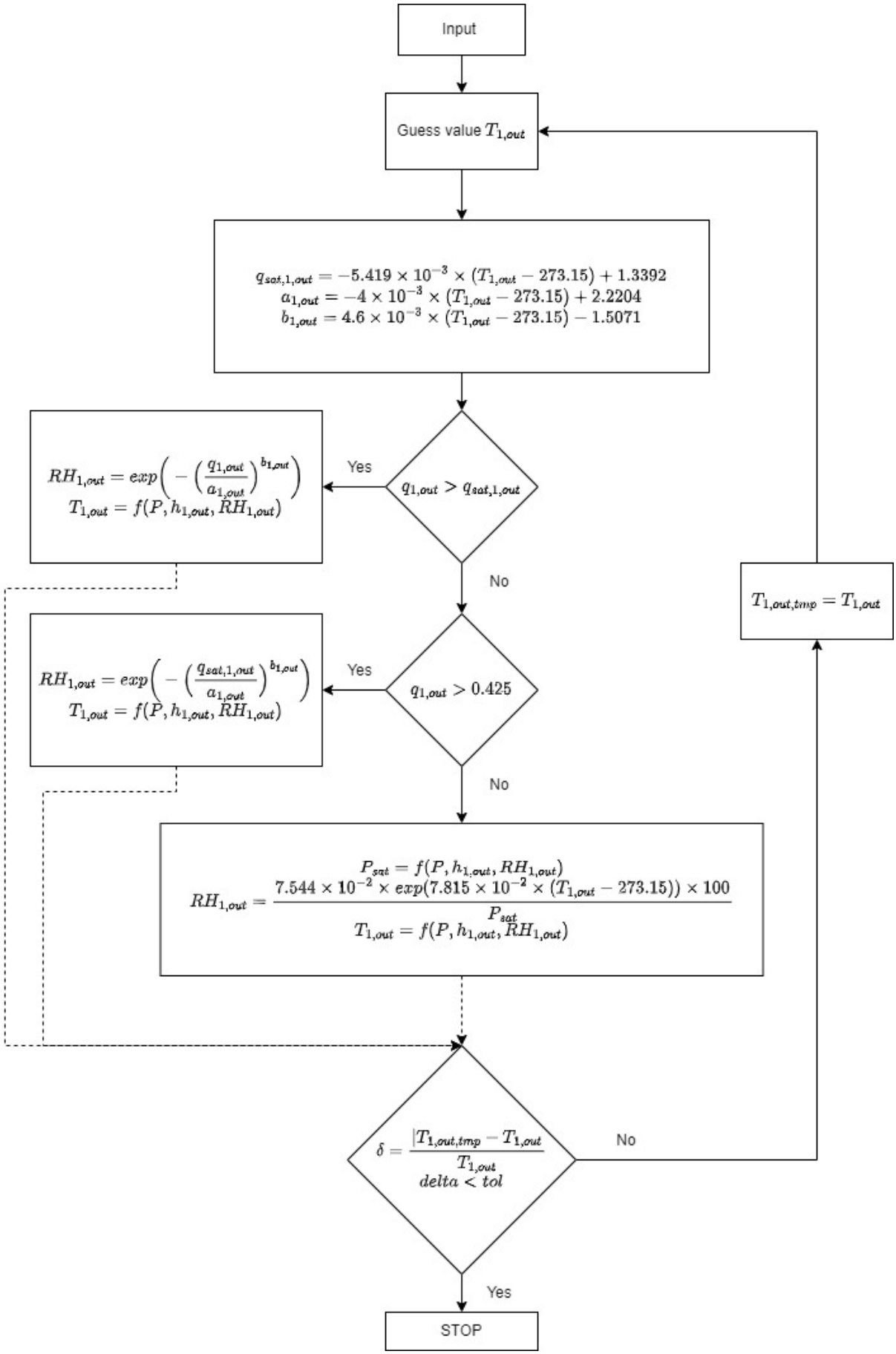

Figure 4.13: Iterative scheme of the complex model of the desiccant wheel to determine the outlet conditions of the wheel.

Parametric analysis

The parameter analysis of the complex model of the desiccant wheel consists in evaluating the importance of the parameter on the output of the model. The only parameter of the complex model is the nominal rotation speed of the wheel $n0$. This nominal value of the parameter given in the *modelica* model is $16[rot/min]$. The corresponding output of the complex model through which the evolution can be seen are the outlet enthalpy $h_{1,out} = h_2$ and specific humidity $w_{1,out} = w_2$ as well as the resulting heat-flow $Q_{s,flow}$ and mass-flow $m_{s,flow}$ rate from the process side to the regeneration side in the desiccant wheel.

The parameter $n0$ evolve from 1.6 to $160[rot/min]$. The evolution is represented on **Figures 4.14** and **4.15**.

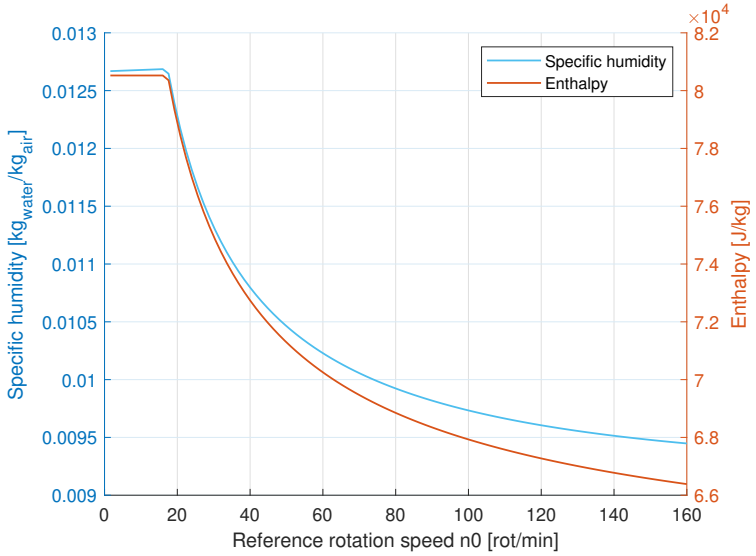

Figure 4.14: Parametric analysis of the desiccant wheel on the outlet conditions of the wheel when the parameter $n0$ evolves.

It can be seen that both, specific humidity and enthalpy curves follow a similar pattern. There is an horizontal curve from zero until the nominal rotation speed and a second order curve after this nominal rotation speed. This sudden change in the curve is due to the conditions in the complex model.

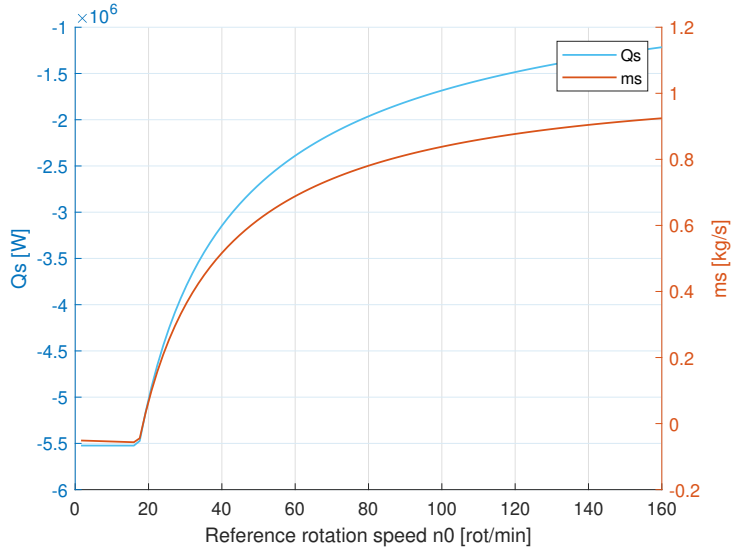

Figure 4.15: Parametric analysis of the desiccant wheel on the resulting heat-flow and the mass-flow rate when the parameter $n0$ evolves.

The second figure follows the same trends. It can be notice that the heat-flow rate is negative meaning that there is more heat after the desiccant wheel in the process side while the mass-flow rate is positive meaning a decrease in specific humidity what was expected.

Calibration and validation

The objective of this section is to evaluate the relevance to use a complete model alongside a simple model. To do this some numerical data are generated from the cycle with complex model for the desiccant evaporative cooling and the rotary air to air exchanger. The external and internal conditions are the weather conditions for the external air and the results of the building model for the internal temperature and the cooling load of the system. Some conditions are deliberately chosen due to a lack of information, these are the internal relative humidity which is fixed at 85% and the regeneration temperature that is fixed to $50°C$ supposing an ideal condition. The data generated only concern the cooling part, i.e. 752 data points.

The evaluation methodology consists in divided the data set into 2 different folds. One for the training, representing 90% of the data set, i.e. 677 values and the second one for the validation with 75 conditions. This distribution of the data set is chosen arbitrary but similar results are obtained with a $50-50\%$ distribution.

Firstly, all the data set generated in save into a table to lead further comparison. The training and validation set are determined randomly by the solver in order to be totally objective.

Secondly, the training data set contains all the input and output conditions of the desiccant wheel generated by the complex model. These data are then used to determine the parameters corresponding to the simple model, equations (4.8, 4.9, 4.10, 4.11). Once these parameters generated, an analysis of these is performed. The distribution of the value of the parameters is respectively represented on **Figure 4.16a** and **Figure 4.16b** for η_{F1} and η_{F2}.

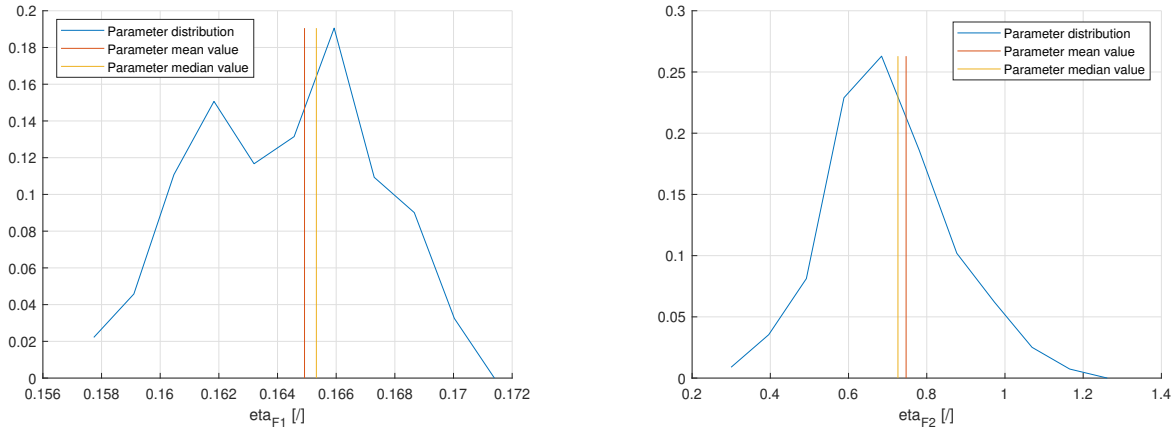

(a) Parameter distribution η_{F1}.

(b) Parameter distribution η_{F2}.

Figure 4.16: Parameter distribution of parameters η_{F1} and η_{F2} with mean median value.

The minimal, mean , median and the maximal value of these parameters are gathered in the **Table 4.4**.

Parameter	Minimal value	Mean value	Median value	Maximal value
η_{F1}	0.1577	0.1649	0.1653	0.1714
η_{F2}	0.2998	0.7472	0.7263	1.2616

Table 4.4: Analysis of parameters generated by the training data set.

The chosen value of the calibration part is the mean value so it comes $\boxed{\eta_{F1} = 0.1649}$ and $\boxed{\eta_{F2} = 0.7472}$.

The third step of the calibration is the validation of the parameter determined previously with validation data set. It consists in evaluating the precision of the use of the simple model with the

design parameters in comparison with the complex model. The output states of the desiccant wheel are determined using the same input conditions than the complex model. This comparison is performed with the 75 operating conditions determined randomly. This numerical validation is illustrated on **Figure 4.17** and **Figure 4.18**, respectively for the output temperature and the output specific humidity.

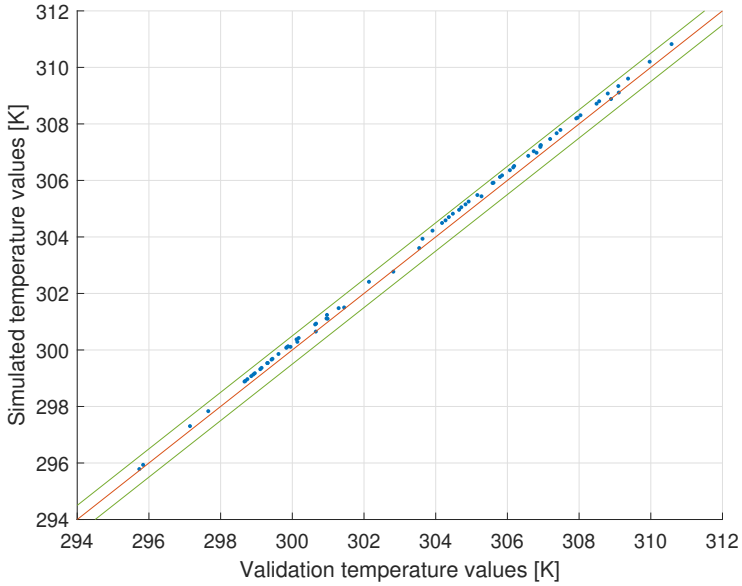

Figure 4.17: Validation and simulated values of the temperature at the process outlet of the desiccant wheel.

The generated data are represented by the blue points on the graph. The figure is also composed of straight lines, in blue is represented the ideal case ($y = x$) while the green lines represent the boundary lines with $+0.5[K]$ and $-0.5[K]$.

The numerical validation of the output specific humidity is represented below :

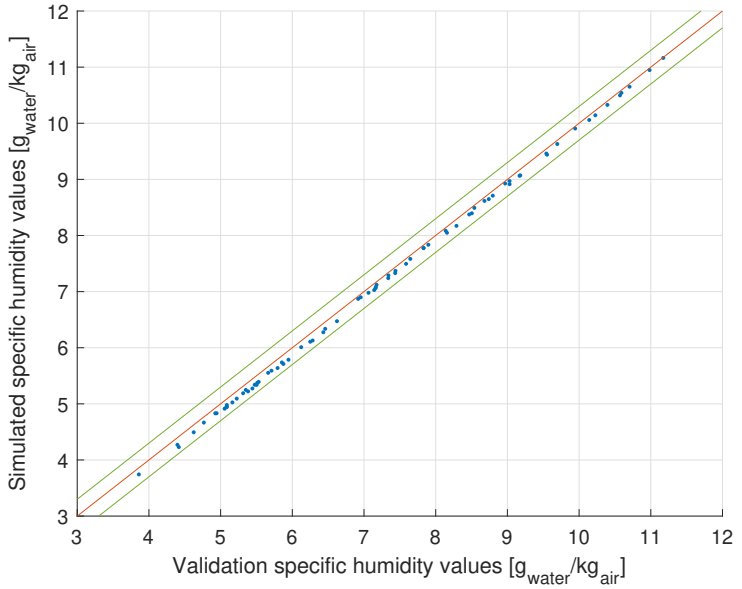

Figure 4.18: Validation and simulated values of the specific humidity at the process outlet of the desiccant wheel.

The legend is similar for **Figure 4.18** as for **Figure 4.17** with green lines representing the a range

from $-0.3[g_{water}/kg_{air}]$ to $+0.3[g_{water}/kg_{air}]$.

The very first conclusion of this validation is that the parameter calibration is really very efficient because the results obtain with the calibrated simple model are almost equal to the generated data with the complex model.

It is also possible to have a quantitative estimation of the error, the difference between the validation and the simulated values both for the temperature and the specific humidity. The root mean square error (RMSE) [23] using equations 4.29 and 4.30 :

$$RMSE_T = \sqrt{\frac{\sum_{j=1}^{n}(T_{j,validation} - T_{j,simulated})^2}{N}} \tag{4.29}$$

$$RMSE_w = \sqrt{\frac{\sum_{j=1}^{n}(w_{j,validation} - w_{j,simulated})^2}{N}} \tag{4.30}$$

In the present case, the obtain values are : $\boxed{RMSE_T = 0.25[K]}$ and $\boxed{RMSE_w = 0.109[g_{water}/kg_{air}]}$. These values are sufficiently small to conclude that the simple model can be used to the detriment of the complex model because the output results are close enough. In an experimental calibration, the measured errors introduced by the different sensors can be higher to these values.

4.2.3 Rotary air to air exchanger

Simple model

For the simple model, the rotary heat exchanger have been modelled as a counter flow heat exchanger with a given efficiency. The corresponding efficiency is described by the following equation :

$$\varepsilon_{HRW} = \frac{\dot{m}_p \times c_p \times (T_2 - T_3)}{\dot{m}_r \times c_p \times (T_2 - T_6)} = \frac{(T_2 - T_3)}{(T_2 - T_6)} \tag{4.31}$$

with equivalent flows in the process and the regeneration sides.

The value of the efficiency of this heat exchanger can be determined based on similar studies. These values are gathered in the **Table 4.5**.

ε_{HRW} [%]	Article
80	[16]
90	[21]
85	[8]
75	[9]

Table 4.5: Heat recovery wheel effectiveness value on different studies.

Parametric study

The only parameter ε_{HRW} have a linear impact on the output temperature while the output specific humidity is constant as there is not mass transfer into the rotary heat exchanger. The input state conditions are gathered in **Table 4.6**.

Point	Temperature $[K]$	Specific humidity $[kg_{water}/kg_{air}]$
2	310	0.01
6	295	0.0162

Table 4.6: Input state conditions of the rotary air to air exchanger for the parametric analysis.

The **Figure 4.19** just below, represents the evolution of the output temperature and the output specific humidity on the process side as a function of the evolution of the parameter ε_{HRW} in a range from 0.5 to 1.

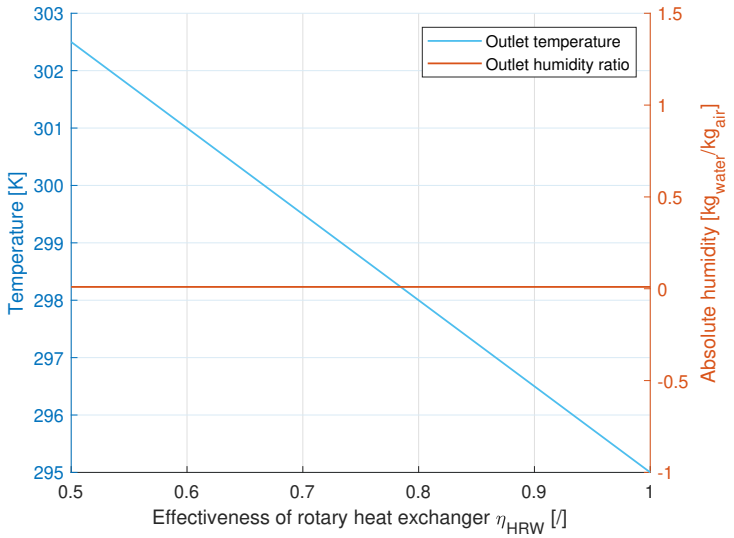

Figure 4.19: Parametric study of the simple rotary air to air heat exchanger when ε_{HRW} evolve.

It can be seen that the output temperature on the process side T_3 decreases when the parameter ε_{HRW} increases. This is the expected result with an ideal heat exchanger and a parameter $\varepsilon_{HRW} = 1$ with maximum transfer of what is physically impossible to have an output temperature equal to the input temperature on the other side.

Complete model

The complex model of the rotary air to air exchanger is provided from a *Modelica* model build by Wrobel et al. [22] in Germany.

The complex model is based on the *Effectiveness - NTU method*. Firstly, it is necessary to determine the heat capacities C_1 and C_2 corresponding to the heat capacity ratio for fluid 1 and 2 respectively the process and the regeneration side of the exchanger. The very first element to introduce is the heat capacity flow W which is defined as the product of the mass flow rate and the heat capacity. So it comes :

$$W_i = \dot{m}_i \times cp_i \tag{4.32}$$

for $i = 1, 2$ respectively for the process and regeneration side of the system. The heat capacity ratio C_1 and C_2 as well as the number of transfer units NTU_1 and NTU_2 are determined following the conditions represented on **Figure 4.20**.

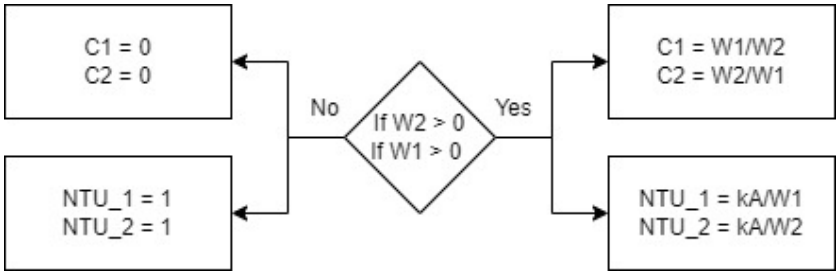

Figure 4.20: Conditions paths for the determination of the heat capacity ratio C_i and the number of transfer units NTU_i.

The second step of the modelling is to determination of the heat exchanger effectiveness. The effectiveness depends on the heat capacity ratio as represented on **Figure 4.21**.

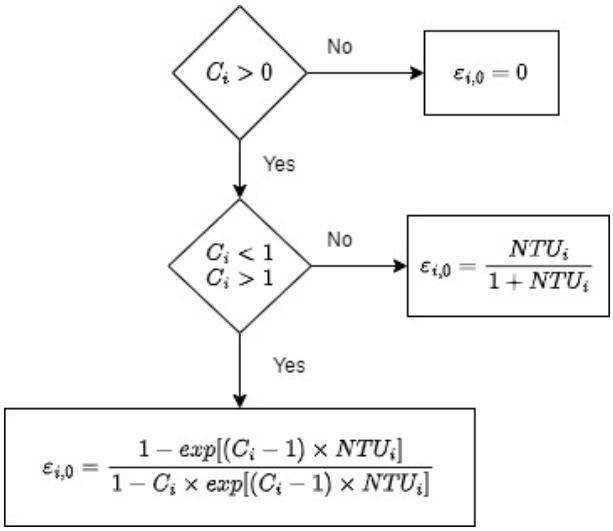

Figure 4.21

To take into account the fact that it is a **rotary** air to air heat exchanger, the influence of the rotation speed have to be taken into account. A correlation is used to correct the model design with

the parameter $n0$ from the variable, the rotation speed of the heat exchanger. This correlation is :

$$a = -0.5136 \times \varepsilon_0 + 0.5136 \tag{4.33}$$

$$\varepsilon = \varepsilon_0 \times \left(\frac{n}{n0} \right)^a \tag{4.34}$$

Finally, the outlet temperature on each side of the exchanger can be determined :

$$T_{1,out} = T_{1,in} - \varepsilon_1 \times (T_{1,in} - T_{2,in}) \tag{4.35}$$

$$T_{2,out} = T_{2,in} - \varepsilon_2 \times (T_{2,in} - T_{1,in}) \tag{4.36}$$

The resulting heat flow from the process side to the regeneration side can be expressed as :

$$Q_{s,flow} = W_1 \times (T_{1,in} - T_{1,out}) \tag{4.37}$$

Parametric study

The parametric study of the complex model of the rotary air to air heat exchanger consists in evaluating the impact of the evolution of the two parameters, the nominal rotation speed of the exchanger $n0$ and the overall heat transfer coefficient UA called kA in the *modelica* modelling, on the output of the model , the outlet temperature on each side of the system which are $T_{1,out} = T_3$ and $T_{2,out} = T_7$ respectively for the process and the regeneration side as well as the resulting heat flow thought the heat exchanger.

The first parameter to evolve is the nominal rotation speed of the heat exchanger $n0$. The nominal value of the parameter is $247.5[rot/min]$. This parameter evolve from 24.75 to $2475[rot/min]$ to evaluate the impact of the parameter on the output of the model while the second parameter kA is kept constant and equal to $500[W/K]$. This first evolution is represented on **Figure 4.22**.

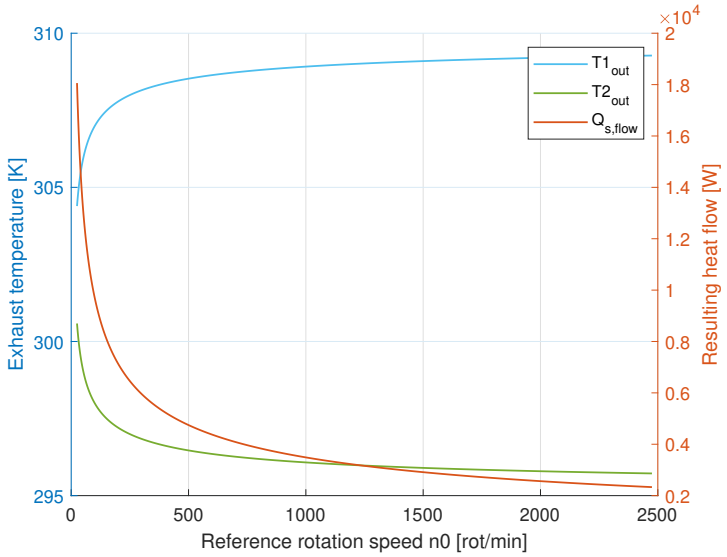

Figure 4.22: Parametric study of the complex model for the rotary air to air heat exchanger when the reference rotation speed evolve and the overall heat transfer coefficient is constant.

It can be noticed that the outlet temperature are symmetrical due to the fact that it is the same fluid at each side with a same flow rate. When the rotation speed parameter increases, the outlet temperature on the process side increases as well, this means that the heat transferred from the process side to the regeneration side decreases when the rotation speed parameter increase. This can be observed on the resulting heat flow which decreases significantly when the reference rotation speed increases.

The second parameter kA evolve from 50 to $5000[W/K]$ while the reference rotation speed is kept constant at $247.5[rot/min]$. This evolution is represented on **Figure 4.23**.

The outlet temperature on the process side $T_{1,out}$ decreases when the heat transfer coefficient increases due to the fact that the heat transfer is easier. This can also be seen on the resulting heat flow which increases when kA increases.

Finally, the reference rotation speed have a higher impact on the output of the model than the heat transfer coefficient.

Calibration and validation

A calibration is performed on the simple model of the rotary air to air heat exchanger in order to use a faster model for simulations. The data used for the calibration and the validation of the model are exactly the same as those used for the desiccant wheel validation. The principle is kept so a data set representing 90% of the all data generated by the complex model is used for the learning part and the

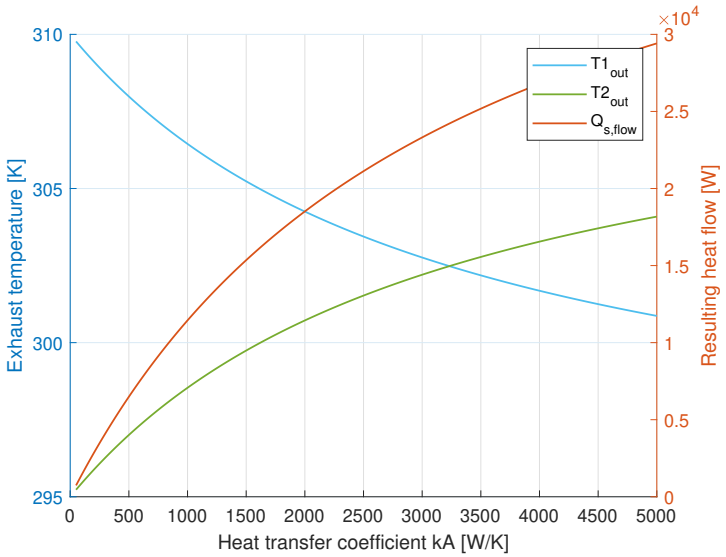

Figure 4.23: Parametric study of the complex model for the rotary air to air heat exchanger when the overall heat transfer coefficient evolve and the reference rotation speed is constant.

remaining 10% are used for the validation.

First of all, a table is created to save all the data generated. Two sub-tables are generated containing the learning and the validation data-set.

In a second step, the corresponding efficiency for all the learning set is determined following the equation 4.41 and save in the corresponding table. With all these parameters, it is possible to generate a distribution figure to evaluate how the parameter is allocated. This distribution is represented on **Figure 4.24**

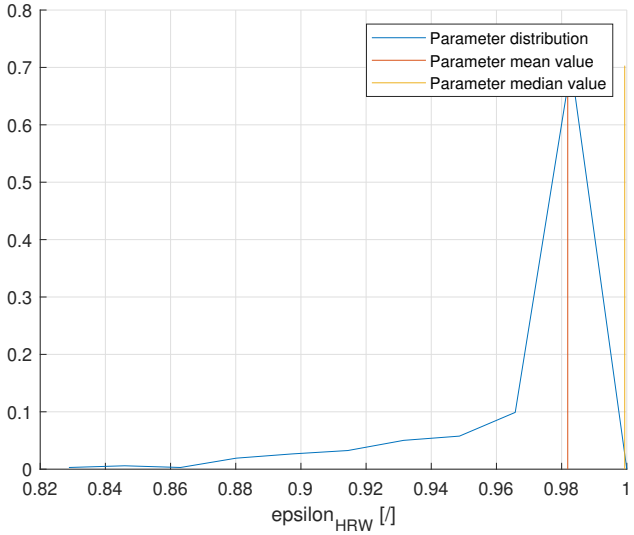

Figure 4.24: Distribution of parameter ε_{HRW} for calibration.

The specific values of this curve is gathered is the **Table 4.7**

It can be notice that the median value is very high so it means that the a half of the value are very close to 1 leading to a perfect heat exchanger. The chosen value is the mean value corresponding to $\boxed{\varepsilon_{HRW} = 0.9819}$. This correspond to a very efficient heat exchanger.

Thirdly, knowing the parameter for the learning, it is necessary to evaluate it with the validation

Parameter	Minimal value	Mean value	Median value	Maximal value
ε_{HRW}	0.8288	0.9819	0.9994	1

Table 4.7: Analysis of parameters generated by the training data set.

set. In the same way as for the desiccant wheel, the output state of the rotary heat exchanger is determined with the validation data set. These output states generated are then compare with the output generated by the complex model. This comparison is represented on the **Figure 4.25**.

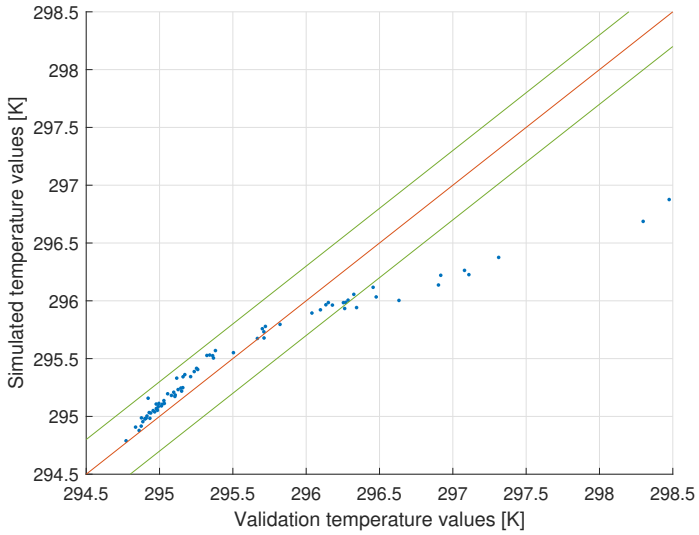

Figure 4.25: Validation and simulated values of temperature at the process outlet of the rotary air to air heat exchanger.

It can be noticed that the data move away from the ideal case ($y = x$) for highest validation temperature values. These values are not included in the boundary lines $-0.3[K]$ and $+0.3[K]$.

After analysing the corresponding data, it can be noticed that the mass flow rate is higher when the validation temperature is high. So further investigation must be performed in order to take into account the mass flow rate with the efficiency equation. When the mass flow rate is to low, the heat exchanger is oversized what is not taken into account into the calibration.

The other validation way is to determined the RMSE value using the equation 4.29. This value is $\boxed{RMSE_T = 0.38[K]}$ which remains a low error in modelling.

4.2.4 Direct evaporative cooler

A Direct Evaporative Cooler (DEC) is a humidifier which sprays water into the air in order to increase is humidity and therefore a drop in temperature. The efficiency of a humidifier is defined as the ratio of the difference between the inlet temperature and the outlet temperature and the inlet temperature and the wet bulb temperature as expressed by equation 4.38.

$$\varepsilon_{DEC} = \frac{T_i - T_o}{T_i - T_{wb,i}} \tag{4.38}$$

In the present case of this study, applying the equation to the state point for the two humidifiers brings :

$$\varepsilon_{EC1} = \frac{(T_3 - T_4)}{(T_3 - T_{wb,3})} \tag{4.39}$$

$$\varepsilon_{EC2} = \frac{(T_5 - T_6)}{(T_5 - T_{wb,5})} \tag{4.40}$$

The values of the efficiency of a direct evaporative cooler from different studies are gathered in the **Table 4.8**

ε_{EC} [%]	Article
85 - 90	[16]
90	[17]

Table 4.8: Direct evaporative cooler effectiveness value from different studies.

Parametric study

The parametric study of the direct evaporative cooler simple model is relatively obvious because the output temperature evolve linearly with the parameter ε_{DEC}. The input state conditions are : $T_{in} = 300K$ and $w_{in} = 0.0111 kg_{water}/kg_{air}$. This study is represented on **Figure 4.26**.

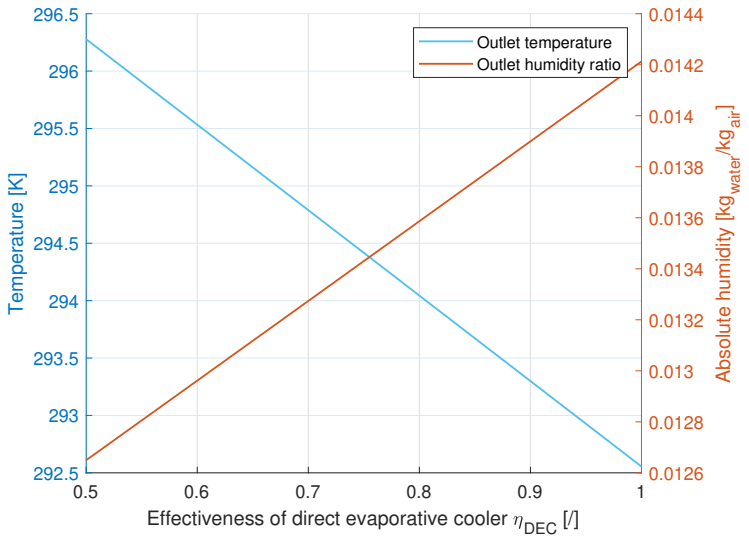

Figure 4.26: Parametric study of the direct evaporative cooler when ε_{DEC} evolves.

I can be seen that when the parameter ε_{DEC} evolve between 0.5 and 1, the output temperature decreases and the specific humidity increases.

4.2.5 Regeneration heat exchanger

The regeneration heat exchanger used to increase the air temperature until a sufficient temperature to lead the regeneration of the desiccant wheel is a counter flow heat exchanger. The exchanger uses hot water from the district network to increase the air temperature.

The regeneration heat exchanger is therefore modelled as a simple heat exchanger with two different fluid on each side. The district heating network provide hot water at $55°C$. The effectiveness ε_{RHE} of the counter flow heat exchanger applied for the study is given below equation 4.41

$$\varepsilon_{RHE} = \frac{C_{air}(T_8 - T_7)}{C_{min}(T_{water,in} - T_7)} \tag{4.41}$$

Where C_{min} and C_{air} are the heat capacities. These terms are developed just after as well as C_{water}.

$$C_{min} = min(C_{air}, C_{water}) \tag{4.42}$$

$$C_{air} = \dot{m}_{air} c_{p,air} \tag{4.43}$$

$$C_{water} = \dot{m}_{water} c_{p,water} = \frac{q}{\Delta T} \tag{4.44}$$

On the water side, the heat capacity is evaluated from the heat use for cooling process at full load which is equal to $\dot{Q}_{water,FL} = 62kW$. Knowing temperatures of the district heating network : heat source temperature $T_{water,in} = 55°$ and heat return temperature $T_{water,out} = 30°$. It is therefore possible to evaluate the maximum heat capacity of water.

$$C_{water} = \dot{m}_{water} c_{p,water} = \frac{\dot{Q}_{water,FL}}{\Delta T} = \frac{62 \times 1000}{55 - 30} = 2480[W/K] \tag{4.45}$$

The specific heat of water $c_{p,water} = 4186[J/kg \cdot K]$ leads to determine the maximum water flow rate passing into the heat exchanger from the district heating network. This flow rate $\dot{m}_{water,MAX} = \frac{2480}{4186} = 0.5925[kg/s]$.

4.3 Conclusion

A first result of the study is the fact that the simple model of the desiccant wheel can substitute the complex model. Even if this model do not described the physical properties of the desiccant wheel it brings with a very high accuracy the outlet of the desiccant wheel. This method must be investigated and applied to a real desiccant evaporative cooling system with experimental data for a complete validation.

Moreover, this simple model can be applied to all desiccant evaporative cooling system whatever the configuration to observe the universality of this model even if it should be compatible as the desiccant wheel have always the same function.

Further investigation must be done on the rotary air to air heat exchanger in order to take into account the air mass flow rate into the effectiveness equation to get closer to reality and to obtain a correct validation of the model.

Chapter 5

Results, discussions and applications

5.1 Results and discussions

The very first result of the modelling is to illustrate the cycle on the psychrometric diagram to observe a real case. The psychrometric diagram is represented on **Figure 5.1**.

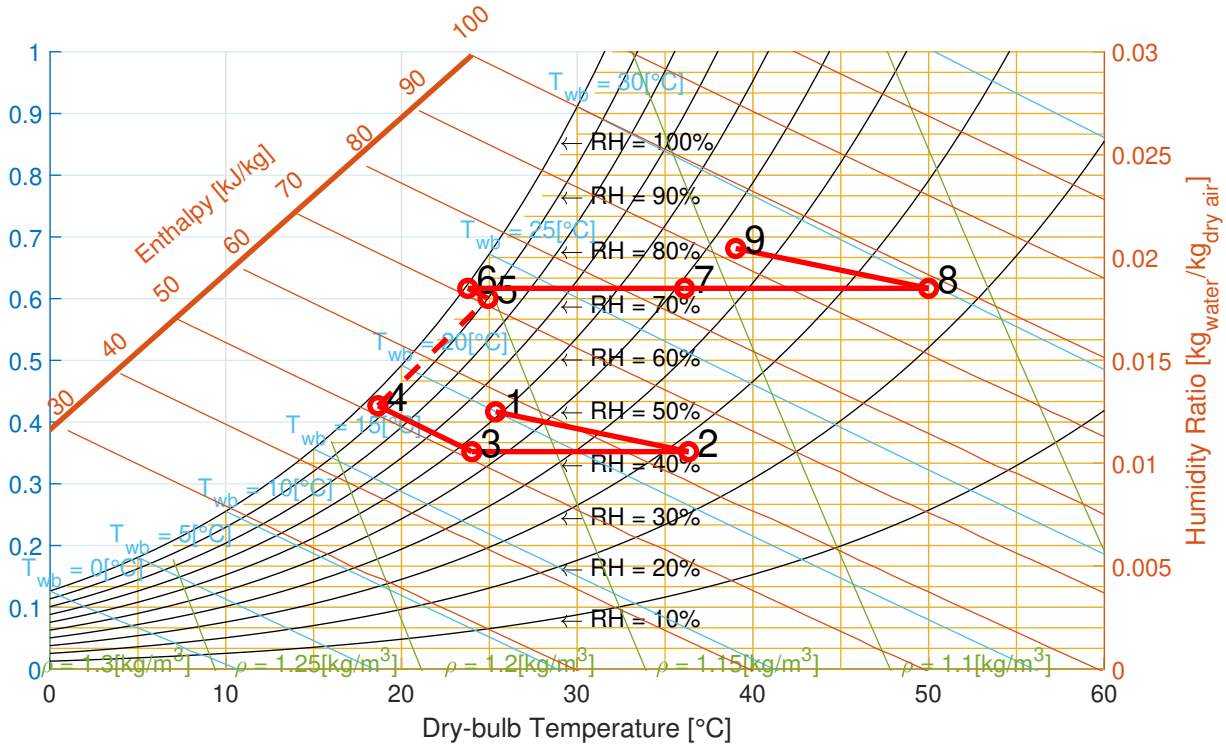

Figure 5.1: Psychometric diagram of the desiccant evaporative cooling system for a typical hour.

The state point 1 representing the external condition of the cycle is determined by the meteorological data at the hour 4600 of the year, which is a typical hour. The internal temperature as well as the cooling load of the desiccant evaporative cooling system is provided by the building model for the same hour. The value of these corresponding points are gathered in the **Table 5.1**.

$T_{out} = T_1[K]$	$\omega_{out} = \omega_1[kg_{water}/kg_{air}]$	$T_{in} = T_5[K]$	$\varphi_{in} = \varphi_5[\%]$	$T_{reg} = T_8[K]$
298.51	0.0125	298.07	90	323.15

Table 5.1: Initial values used corresponding to the typical hour 4600.

The parameters used for the modelling is also gathered in the **Table 5.2**.

The performance of the desiccant evaporative cooling system is expressed by the coefficient of performance *COP*. Two different COP can be defined as described by Elgendy et al. [5]. The thermal

$\varepsilon_{DEC}[/]$	$\varepsilon_{DHRW}[/]$	$\eta_{F1}[/]$	$\eta_{F2}[/]$
0.9	0.9819	0.1649	0.7472

Table 5.2: Parameters obtained by the calibration of the simple model.

coefficient of performance COP_{th} and the air handling coefficient of performance COP_d. COP_{th} is defined as the ratio of space cooling capacity to the regeneration energy rate while COP_d represents the ratio of the rate of air handling capacity to the required regeneration energy rate and can be estimated as :

$$COP_{th} = \frac{Q_{cool}}{Q_{reg}} = \frac{\dot{m}_a(h_5 - h_4)}{\dot{m}_a(h_8 - h_7)} \tag{5.1}$$

$$COP_d = \frac{Q_d}{Q_{reg}} = \frac{\dot{m}_a(h_1 - h_4)}{\dot{m}_a(h_8 - h_7)} \tag{5.2}$$

In the present case, these performance are : $\boxed{COP_{th} = 1.3637[/]}$ and $\boxed{COP_d = 0.4254[/]}$. The air mass flow rate into the system is $\boxed{\dot{m}_{air} = 2.7189[kg/s]}$ and the water consumption is : $\boxed{\dot{m}_{water} = 7.4[g_{water}/s]}$. This last value is realist knowing that the water use for cooling process at full load is $81L/h$ according to [2].

It t can be interesting to observe the evolution of the Coefficient Of Performance (COP) when the external temperature and the external humidity ratio evolve.

When the temperature evolve, the humidity ratio is kept constant. It is important to be careful to the fact that it is well the humidity ratio with the unit $[kg_{water}/kg_{air}]$ that is constant and not the relative humidity in $[\%]$ because the last one is linked to the temperature as it can be seen on a psychrometric diagram **Figure 5.1** . The temperature evolve from 20 to 40 $°C$ for a constant humidity ratio $0.0125[kg_{water}/kg_{air}]$. The other conditions are the already mentioned in **Table 5.1**.

The evolution of the both COP when the external temperature increases is illustrated on **Figure 5.2**.

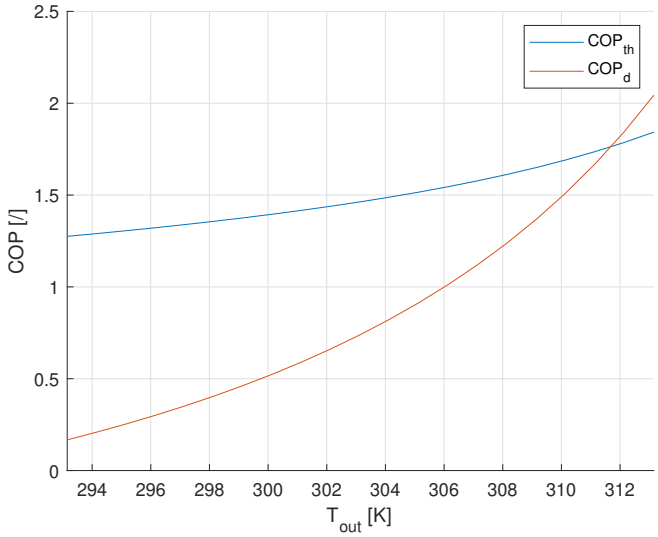

Figure 5.2: Evolution of the COP_{th} and COP_d when the external temperature increases.

It can be seen that the thermal coefficient of performance increases when the external temperature increases. This is not an expected solution and this is in contradiction with the results obtained by Elgendy et al. [5] in their article. When the external temperature increases, the expected result is a decrease in the thermal coefficient of performance because the system has more difficulty to cool

a room when it uses high temperature. This inconsistency could provide from the rotary air to air effectiveness which too close to the ideal case which in practice leads to have an outlet temperature on the process side that is very close to the inlet temperature on the regeneration side, respectively T_3 and T_6. As the internal temperature and relative humidity in the room is supposed constant, consequently the temperature T_3 and so T_4 is relatively constant when the external temperature evolve. In the same way, the outlet temperature on the process side T_7 is very similar to the inlet temperature T_2 which varies with the external temperature. There is on the internal side a relatively constant heat transfer rate $h_5 - h_4$ while on the external side the enthalpy difference $h_8 - h_7$ decreases as the state point 8 is constant and the state point temperature T_7 increases with the external temperature.
This can be proved by a same analysis but with a different rotary air to air effectiveness. For example, in order to have a significant impact, the rotary air to air heat exchanger effectiveness is fixed ε_{HRW} = 0.7. All the other parameters are kept constant and the simulation conditions are the same. This new **Figure 5.3** is represented below.

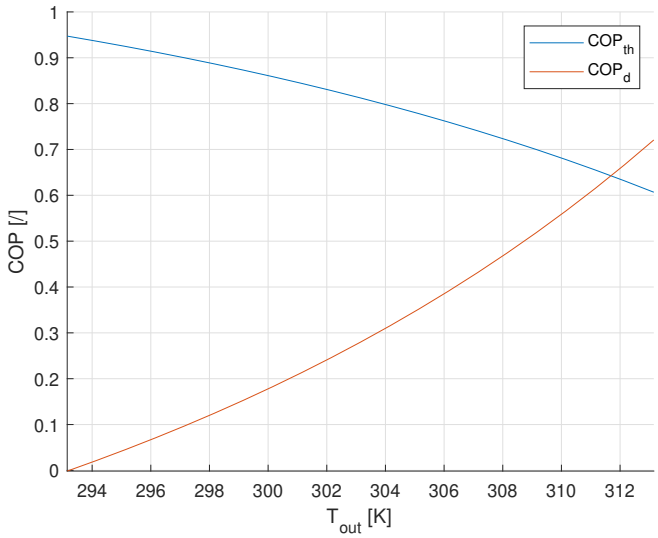

Figure 5.3: Evolution of the COP_{th} and COP_d when the external temperature increases for ε_{HRW} = 0.7.

It can be observed that in this case, with a effectiveness ε_{HRW} = 0.7, the thermal coefficient of performance decreases when the external temperature increases. This proves the impact of the this parameter on the global performance of the wheel.

In a second time, it is the humidity ratio which evolve. The humidity ratio varies from 0.006 to 0.02$[kg_{water}/kg_{air}]$ and the external temperature is kept constant at 25.36°. The evolution is represented on **Figure 5.4**.

It can be notice that the thermal coefficient of performance decreases when the humidity ratio increases what could be expected as when the air has a high moisture content, the evaporation effect is low. The desiccant wheel work increases with the humidity ratio what increases the energy consumption and therefore the thermal coefficient of performance. In addition to this, the air handling coefficient of performance increases with the humidity ratio because the enthalpy difference between the inlet and the outlet of the process side increases faster than the regeneration power.

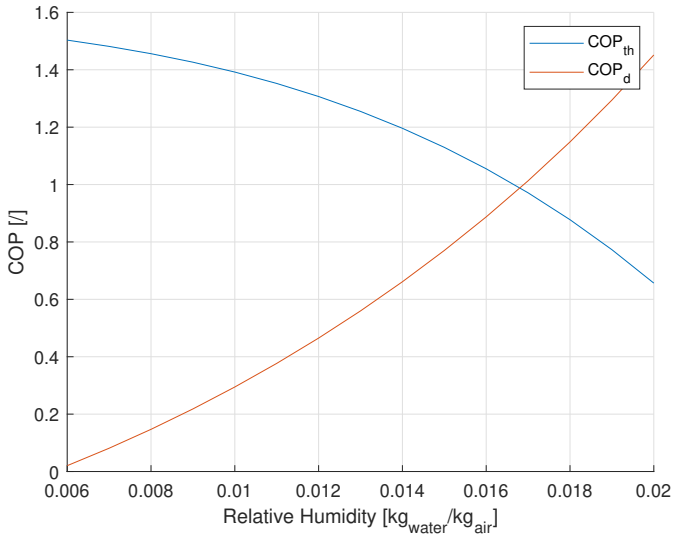

Figure 5.4: Evolution of the COP_{th} and COP_d when the external humidity ratio increases.

5.2 Applications

The desiccant evaporative cooling system is a very interesting alternative for air cooling. This system can substitute conventional air conditioning unit with a compressor which consumes a lot of electricity because the electricity consumption of this technology is relatively low.

Most of studies mentioned in the literature review proposed to apply this technology in hot and humid climate in combination with solar collectors for the regeneration load. The most important need for cold air takes place in summer during the day, it is also when the sun has the higher irradiation so this energy is available. In addition this energy is free so it is very interesting for developing countries because the impact of such technology is relatively low in comparison with a conventional air cooler with compressor (high electric consumption).

An important element to mention is that when the COP is evaluated between the desiccant evaporative cooling system and the conventional air cooler, the primary energy used are different between the two systems. The desiccant evaporative cooling system uses heat to increase the air temperature for the regeneration while the conventional air conditioning consumes electricity which are two different energetic vectors with different levels of values.

In the case of the CREATE building, the heating district network is used to reach the regeneration temperature. Heat from the network is relatively cheap during summer because the heating demand is at its minimum. The direct connection to the district heating network presents an advantage due to the under-used of the district during summer and reduce the load on the electricity grid. Furthermore, this allow local industries to inject a larger share of heat surplus into the district heating grid during the cooling season.

This technology has a very large range of design which leads to several applications. For example, the recirculation cycle system can be used for data center cooling in combination with an indirect evaporative cooler because there is need of a very dry air. The standard configuration is better suited for living room for sanitary reasons.

For hot and humid countries, the desiccant evaporative cooling system is a real opportunity to enable the space cooling with a relatively low energy cost. Moreover when the regeneration temperature is reached with solar collectors which means a renewable and free energy.

Chapter 6

Conclusion

In this study, the desiccant evaporative cooling system has been analysed.

In a fist step, the description of the modelling is carried out with an analysis of the cycle on the psychrometric diagram.

Secondly, a literature review including the different configuration of such system. Both the flux configuration and the alternative to direct evaporative cooling for standard cycle are reviewed. The modelling of the different components, the desiccant wheel and the evaporative cooler is also reviewed. The performance and the applications of such technology in the literature is tackled.

The modelling of the complete cycle is the third step of this study. The building modelling is realised from a simplified model to determine the temperature and cooling load of the building. The cycle model with an iterative scheme gathering all the components is illustrated. The modelling, simple and complex, for each component is done with a parametric analysis. For the desiccant wheel and the rotary air to air heat exchanger, the calibration and the validation is performed to evaluate the compatibility of these model on a same component. The simple model of the desiccant wheel can substitute the complex model for further modelling due to a high correspondence between the simulated and the validation values

Finally, results and discussions from the complete system for a particular point is done. An analysis on the influence of the external temperature as well as the external humidity ratio is realised to observe the evolution of COP. The possible applications of such technology is tackled to illustrate the potential of this technology.

Bibliography

[1] M. Mujahid Rafique, P. Gandhidasan, Shafiqur Rehman, and Luai M.Al-Hadhrami. A review on desiccant based evaporative cooling systems. *Renewable and Sustainable Energy Reviews*, 45:145–159, 2015. https://doi.org/10.1016/j.rser.2015.01.051.

[2] Hicham Johra. Instant district cooling system : Project study case presentation, 2021. https://vbn.aau.dk/en/publications/instant-district-cooling-system-project-study-case-presentation.

[3] K. Daou, R.Z. Wang, and Z.Z. Xia. Desiccant cooling air conditioning: a review. *Renewable and Sustainable Energy Reviews*, 10:55–77, 2006. https://doi.org/10.1016/j.rser.2004.09.010.

[4] Muzaffar Ali, Vladimir Vukovic, Nadeem Ahmed Sheikh, and Hafiz M.Alib. Performance investigation of solid desiccant evaporative cooling system configurations in different climatic zones. *Energy Conversion and Management*, 97:323–339, 2015. https://doi.org/10.1016/j.enconman.2015.03.025.

[5] E.Elgendy, A.Mostafa, and M.Fatouh. Performance enhancement of a desiccant evaporative cooling system using direct/indirect evaporative cooler. *International Journal of Refrigeration*, 51:77–87, 2015. https://doi.org/10.1016/j.ijrefrig.2014.12.009.

[6] S. Jain, P.L. Dhar, and S.C. Kaushik. Evaluation of solid-desiccant-based evaporative cooling cycles for typical hot and humid climates. *International Journal of Refrigiration*, 18(5):287–296, 1995. https://doi.org/10.1016/0140-7007(95)00016-5.

[7] Yunus Emre Güzelel, Umutcan Olmuş, and Orhan Büyükalaca. Simulation of a desiccant air-conditioning system integrated with dew-point indirect evaporative cooler for a school building. *Applied Thermal Engineering*, 217(119233), 2022. https://doi.org/10.1016/j.applthermaleng.2022.119233.

[8] Lanbo Lai, Xiaolin Wang, Gholamreza Kefayati, and Eric Hub. Performance evaluation of a solar powered solid desiccant evaporative cooling system with different recirculation air ratios. *Energy and Buildings*, 270(112273), 2022. https://doi.org/10.1016/j.enbuild.2022.112273.

[9] Ghulam Qadar Chaudhary, Muzaffar Ali, Nadeem Ahmed Sheikh, Syed Ihtsham ul Haq Gilani, and Shahab Khushnood. Integration of solar assisted solid desiccant cooling system with efficient evaporative cooling technique for separate load handling. *Applied Thermal Engineering*, 140:696–706, 2018. https://doi.org/10.1016/j.applthermaleng.2018.05.081.

[10] Liu Chen, Yujie Chu, and Wenjie Deng. Experimental investigation of dedicated desiccant wheel outdoor air cooling systems for nearly zero energy buildings. *International Journal of Refrigeration*, 134:265–277, 2022. https://doi.org/10.1016/j.ijrefrig.2021.11.016.

[11] D.B. Jani, Manish Mishra, and P.K. Sahoo. Solid desiccant air conditioning – a state of the art review. *Renewable and Sustainable Energy Reviews*, 60:1451–1469, 2016. https://doi.org/10.1016/j.rser.2016.03.031.

[12] Seiichi Yamaguchi and Kiyoshi Saito. Numerical and experimental performance analysis of rotary desiccant wheels. *International Journal of Heat and Mass Transfer*, 60:51–60, 2013. https://doi.org/10.1016/j.ijheatmasstransfer.2012.12.036.

[13] G.Panaras, E.Mathioulakis, V.Belessiotis, and N.Kyriakisb. Experimental validation of a simplified approach for a desiccant wheel model. *Energy and Buildings*, 42(10):1719–1725, 2010. https://doi.org/10.1016/j.enbuild.2010.05.006.

[14] Fatemeh Esfandiari Nia, Dolf van Paassen, and Mohamad Hassan Saidi. Modeling and simulation of desiccant wheel for air conditioning. *Energy and Buildings*, 38(10):1230–1239, 2006. https://doi.org/10.1016/j.enbuild.2006.03.020.

[15] A. Fouda and Z. Melikyan. A simplified model for analysis of heat and mass transfer in a direct evaporative cooler. *Applied Thermal Engineering*, 31(5):932–936, 2011. https://doi.org/10.1016/j.applthermaleng.2010.11.016.

[16] M. Mujahid Rafique, P. Gandhidasan, Shafiqur Rehman, and Luai M.Alhems. Performance analysis of a desiccant evaporative cooling system under hot and humid conditions. *Environmental Progress Sustainable Energy*, 35(5), 2016. https://doi.org/10.1002/ep.12358.

[17] Yunlong Ma and Lisa Guan. Performance analysis of solar desiccant-evaporative cooling for a commercial building under different australian climates. *Procedia Engineering*, 121:528–535, 2015. https://doi.org/10.1016/j.proeng.2015.08.1024.

[18] Leila Merabti, Mustapha Merzouk, Nachida Kasbadji Merzouk, and Walid Taane. Performance study of solar driven solid desiccant cooling system under algerian coastal climate. *International Journal of Hydrogen Energy*, 42(48):28997–29005, 2017. https://doi.org/10.1016/j.ijhydene.2017.08.067.

[19] D.C. Hittle. *Calculating building heating and cooling loads using the frequency response of multilayered slabs*. Construction engineering research laboratory, Illinois, 1981.

[20] http://www.energia.ae/desiccant-wheel.html.

[21] Amirreza Heidaria, Ramin Roshandela, and Vahid Vakiloroayab. An innovative solar assisted desiccant-based evaporative cooling system for co-production of water and cooling in hot and humid climates. *Energy Conversion and Management*, 185:396–409, 2019. https://doi.org/10.1016/j.enconman.2019.02.015.

[22] Jan Wrobel, Paula Morgenstern, and Gerhard Schmitz. Modeling and experimental validation of the desiccant wheel in a hybrid desiccant air conditioning system. *Applied Thermal Engineering*, pages 1082–1091, 2013. https://doi.org/10.1016/j.applthermaleng.2012.09.033.

[23] Bertrand Cornélusse. ELEN0445-1 : Microgrids.